

Doctorate Program in Molecular
Oncology and Endocrinology
Doctorate School in Molecular
Medicine

XXIII cycle - 2007–2010
Coordinator: Prof. Giancarlo Vecchio

**“Inside the function of the 67 kDa laminin receptor
(67LR): a new promising target for cancer drug discovery
by structure-based virtual screening”**

Ada Pesapane

University of Naples Federico II
Dipartimento di Biologia e Patologia Cellulare e
Molecolare
“L. Califano”

Administrative Location

Dipartimento di Biologia e Patologia Cellulare e Molecolare “L. Califano”
Università degli Studi di Napoli Federico II

Partner Institutions

Italian Institutions

Università degli Studi di Napoli “Federico II”, Naples, Italy
Istituto di Endocrinologia ed Oncologia Sperimentale “G. Salvatore”, CNR,
Naples, Italy
Seconda Università di Napoli, Naples, Italy
Università degli Studi di Napoli “Parthenope”, Naples, Italy
Università del Sannio, Benevento, Italy
Università di Genova, Genoa, Italy
Università di Padova, Padua, Italy
Università degli Studi “Magna Graecia”, Catanzaro, Italy
Università degli Studi di Firenze, Florence, Italy
Università degli Studi di Bologna, Bologna, Italy
Università degli Studi del Molise, Campobasso, Italy
Università degli Studi di Torino, Turin, Italy
Università di Udine, Udine, Italy

Foreign Institutions

Université Libre de Bruxelles, Brussels, Belgium
Universidade Federal de Sao Paulo, Brazil
University of Turku, Turku, Finland
Université Paris Sud XI, Paris, France
University of Madras, Chennai, India
University Pavol Jozef Šafárik, Kosice, Slovakia
Universidad Autonoma de Madrid, Centro de Investigaciones Oncologicas
(CNIO), Spain
Johns Hopkins School of Medicine, Baltimore, MD, USA
Johns Hopkins Krieger School of Arts and Sciences, Baltimore, MD, USA
National Institutes of Health, Bethesda, MD, USA
Ohio State University, Columbus, OH, USA
Albert Einstein College of Medicine of Yeshiwa University, N.Y., USA

Supporting Institutions

Associazione Leonardo di Capua, Naples, Italy

Dipartimento di Biologia e Patologia Cellulare e Molecolare “L. Califano”,
Università degli Studi di Napoli “Federico II”, Naples, Italy
Istituto Superiore di Oncologia (ISO), Genoa, Italy
Istituto di Endocrinologia ed Oncologia Sperimentale “G. Salvatore”, CNR,
Naples, Italy

Italian Faculty

Giancarlo Vecchio, MD, Co-ordinator
Salvatore Maria Aloj, MD
Francesco Saverio Ambesi Impiombato, MD
Francesco Beguinot, MD
Maria Teresa Berlingieri, MD
Bernadette Biondi, MD
Francesca Carlomagno, MD
Gabriella Castoria, MD
Angela Celetti, MD
Lorenzo Chiariotti, MD
Vincenzo Ciminale, MD
Annamaria Cirafici, PhD
Annamaria Colao, MD
Sabino De Placido, MD
Gabriella De Vita, MD
Monica Fedele, PhD
Pietro Formisano, MD
Alfredo Fusco, MD
Michele Grieco, MD
Massimo Imbriaco, MD
Paolo Laccetti, PhD
Antonio Leonardi, MD
Paolo Emidio Macchia, MD
Barbara Majello, PhD
Rosa Marina Melillo, MD
Claudia Miele, PhD
Roberto Pacelli, MD
Giuseppe Palumbo, PhD
Silvio Parodi, MD
Nicola Perrotti, MD
Giuseppe Portella, MD
Giorgio Punzo, MD
Antonio Rosato, MD
Guido Rossi, MD
Giuliana Salvatore MD
Massimo Santoro, MD
Giampaolo Tortora, MD
Donatella Tramontano, PhD
Giancarlo Troncone, MD
Giuseppe Viglietto, MD
Mario Vitale, MD

Foreign Faculty

Université Libre de Bruxelles, Belgium

Gilbert Vassart, MD
Jacques E. Dumont, MD

Universidade Federal de Sao Paulo, Brazil

Janete Maria Cerutti, PhD
Rui Monteiro de Barros Maciel, MD PhD

University of Turku, Turku, Finland

Mikko Laukkanen, PhD

Université Paris Sud XI, Paris, France

Martin Schlumberger, MD
Jean Michel Bidart, MD

University of Madras, Chennai, India

Arasambattu K. Munirajan, PhD

University Pavol Jozef Šafàrik, Kosice, Slovakia

Eva Cellárová, PhD
Peter Fedoročko, PhD

Universidad Autonoma de Madrid - Instituto de Investigaciones Biomedicas, Spain

Juan Bernal, MD, PhD
Pilar Santisteban, PhD

Centro de Investigaciones Oncologicas, Spain

Mariano Barbacid, MD

Johns Hopkins School of Medicine, USA

Vincenzo Casolaro, MD
Pierre A. Coulombe, PhD
James G. Herman MD
Robert P. Schleimer, PhD

Johns Hopkins Krieger School of Arts and Sciences, USA

Eaton E. Lattman, MD

National Institutes of Health, Bethesda, MD, USA

Michael M. Gottesman, MD
J. Silvio Gutkind, PhD
Genoveffa Franchini, MD
Stephen J. Marx, MD
Ira Pastan, MD
Phillip Gorden, MD

Ohio State University, Columbus, OH, USA

Carlo M. Croce, MD
Ginny L. Bumgardner, MD PhD

Albert Einstein College of Medicine of Yeshiwa University, N.Y., USA

Luciano D'Adamio, MD
Nancy Carrasco, MD

**“Inside the function of the 67
kDa laminin receptor (67LR):
a new promising target for
cancer drug discovery by
structure-based virtual
screening”**

TABLE OF CONTENTS

1 INTRODUCTION	5
1.1 The 67 kDa laminin receptor (67LR): structure and function.....	5
1.2 67LR in tumor invasion and metastasis.....	6
1.3 67LR crystal structure.....	7
1.4 Phosphoprotein enriched in diabetes/phosphoprotein enriched in astrocytes-15 kDa (PED/PEA-15): structure and function.....	9
1.5 PED/PEA-15 in tumorigenesis and cancer progression.....	10
1.6 Structure-based drug design by “virtual screening”.....	11
2 AIM OF THE STUDY.....	13
3 MATERIALS AND METHODS.....	14
3.1 Materials.....	14
3.2 Transformation of Yeast Strains and β -Galactosidase Assay	14
3.3 Cell culture.....	14
3.4 Transfection.....	14
3.5 Flow cytometric analysis of surface molecules.....	15
3.6 Western blot.....	15
3.7 PED/PEA-15/67LR interaction.....	15
3.8 Coimmunoprecipitation	16
3.9 Rac1 pull-down assay.....	16
3.10 Adhesion Assay.....	16
3.11 Cell proliferation assay.....	16
3.12 Cell apoptosis assay	17
3.13 Cell Migration Assay	17
3.14 Invasion assay	17
3.15 Statistical analysis	18
4 RESULTS AND DISCUSSION.....	19
4.1 Isolation and identification of 37 kDa laminin receptor precursor (37LRP) as a novel PED/PEA-15 interacting protein	19
4.2 67LR interacts with PED/PEA-15 in vitro as well as in mammalian cells	19
4.3 PED/PEA-15 overexpression increases 67LR-mediated cell adhesion and migration/invasion toward laminin	21
4.4 PED and 67LR interaction increases cell migration/invasion toward laminin and affects ECM signaling	22
4.5 Cell adhesion to LM allows cell proliferation in PED/PEA-15 overexpressing cells by modulating PED/PEA-15 phosphorylation status	24
4.6 Cell adhesion to LM also inhibits apoptosis in PED/PEA-15 overexpressing cells.....	26
4.7 Cell adhesion to laminin regulates PED-PEA-15 phosphorylation by activating protein Kinase C and calcium/calmodulin-dependent protein Kinase II	27
4.8 Virtual screening of a diversity library of small molecules on 67LR	28

4.9	37LRP cDNA transfection in HEK-293 cells results in cell surface expression of the mature receptor and increased cell adhesion to laminin	29
4.10	LR-293 cell adhesion to laminin is inhibited by molecules selected by Virtual Screening.....	30
4.11	A molecule identified by a virtual screenig is a specific inhibitor of 67LR binding to laminin	31
4.12	NSC47924 is a specific inhibitor of 67LR –mediated cell binding to laminin and shows an I_{c50} in the μ molar range.....	32
4.13	The specific 67LR inhibitor NSC47924 inhibitis cell proliferation, migration and invasion in response to laminin	33
5	CONCLUSION.....	34
6	REFERENCES	36

LIST OF PUBLICATIONS

This dissertation is based upon the following publications:

Montuori N, Bifulco K, Carriero MV, La Penna C, Visconte V, Alfano D, Pesapane A, Rossi FW, Salzano S, Rossi G, Ragno P. The cross-talk between the urokinase receptor and fMLP receptors regulates the activity of the CXCR4 chemokine receptor. *Cell Mol Life Sci*. 2010 Oct 24. [Epub ahead of print].

Formisano P, Ragno P, Pesapane A, Giusto R, Alfano D, Rea VEA, Beguinot F, Rossi G, Montuori N. PED/PEA-15 interacts with the 67kDa laminin receptor and regulates cell adhesion, migration, proliferation and apoptosis in response to laminin. Manuscript in preparation.

ABSTRACT

The 67 kDa laminin receptor (67LR) is a non-integrin cell-surface receptor for the extracellular matrix derived from the dimerization of a 37 kDa cytosolic precursor (37LRP). 67LR is highly expressed in human cancers and widely recognized as a molecular marker of metastatic aggressiveness.

Phosphoprotein enriched in diabetes/phosphoprotein enriched in astrocytes (PED/PEA-15) is an anti-apoptotic protein whose expression is increased in several human cancers. In addition to apoptosis, PED/PEA-15 is involved in the regulation of other major cellular functions, including cell adhesion, migration, proliferation and glucose metabolism.

A yeast two-hybrid screening identified 67LR as a PED/PEA-15 interacting partner. PED/PEA-15 molecular interaction with 67LR was confirmed by pull-down experiments on lysates of PED/PEA-15 transfected HEK-293 cells. Overexpressed and endogenous PED/PEA-15 co-immunoprecipitated with 67LR in PED/PEA-15 transfected HEK-293 cells and in U-373 glioblastoma cells, respectively.

PED/PEA-15 overexpression significantly increased 67LR-mediated HEK-293 cell adhesion and migration to laminin that, in turn, determined PED/PEA-15 phosphorylation both in Ser-104 and Ser-116, through CamKII and PKC activation, thus enabling cell proliferation and resistance to apoptosis.

Therefore, 67LR binding to laminin induces, through interaction with PED/PEA-15, signals that may be crucial for tumor cell survival in a poor microenvironment. Indeed, high 67LR expression predicts for a more aggressive disease in several types of cancer.

These considerations prompted us to search for small molecules that might target 67LR activities. Since cancer cells overexpress 67LR, these compounds are expected to be cancer cell specific and minimally toxic. We conducted a computational screening of a diversity library of small molecules using the recently solved 67LR crystal structure, focusing on residues showed to be important for laminin binding. This analysis identified a lead compound that was characterized for its effects. This lead compound, NSC47924, could be the basis for the development of a new class of anti-cancer drugs, specifically targeting tumor invasion and metastasis.

1. INTRODUCTION

1.1 *The 67 kDa laminin receptor (67LR): structure and function*

The 67 kDa laminin receptor 67LR was originally identified as a non-integrin cell surface receptor for the extracellular matrix molecule laminin (Rao 1983). Laminins, other glycoproteins, collagen IV, and proteoglycans constitute a tight network to form the basement membrane. Laminin-1, a 900-kDa glycoprotein, is the major component of basement membranes and contains many bioactive domains involved in binding both integrin and nonintegrin receptors (Mecham 1991). Interactions between 67LR and laminin play a major role in mediating changes in the cellular environment that affect cell adhesion (Graf 1987), neurite outgrowth (Mecham 1991), tumor growth and metastasis (Taraboletti 1993).

67LR has been observed to act also as a cell surface receptor for the pathogenic prion protein (Gauczynski 2001) and a variety of viruses, including Sindbis virus (Nelson 2008).

67LR derives from homo- or hetero-dimerization of a 37 kDa cytosolic precursor, the 37LRP (Rao 1989). The exact composition of the 67kDa dimer and the process by which it is formed from 37LRP remains obscure as evidence supports both a homo and a heterodimer (Scheiman et al 2010). 67LR was shown to be acylated by three fatty acids- palmitate, stearate and oleate - (Landowski et al 1995) and fatty acid synthesis is required for 67LR formation (Butò et al 1998).

Interestingly, both human 67LR and the p40 ribosomal protein are encoded by the same gene, 37LRP/p40 (Jackers 1996). Sequence conservation of 37LRP/p40 genes across species has been demonstrated, with evolution of the C-terminal tail, where is located the laminin binding domain, convergent with vertebrates (Ardini 1998). Thus, human 37LRP shows a dual function, as a component of the translational machinery and as a precursor a cell surface receptor, which suggests that 37LRP is a multifunctional protein. Intracellular 37LRP is found on the 40S ribosome and polysomes (Ford 1999; Auth 1992) and in the nucleus (Kinoshita 1998). Silencing 37LRP expression in mammalian cells induces G1 cell cycle arrest, protein translation shutdown, and loss of association with the polysomes (Scheiman 2010).

67LR is located at the cell surface where it binds laminin through different binding domains, including residues 161–180 (peptide G), residues 205–229 and TEDWS-containing C-terminal repeats (Castronovo 1991; Kazmin 2000). Laminin conformation changes upon binding 67LR, thus interacting more efficiently with integrins (Magnifico 1996), becoming more sensitive to the action of proteolytic enzymes (Ardini 2002) and releasing motility fragments (Berno 2005).

67LR is co-expressed and can physically interact with the α_6 integrin chain (Ardini 1997).

The minimal sequence of laminin that binds to 67LR is YIGSR, a pentapeptide localized on the short arm of the laminin, just below the cross intersection (Massia 1993).

Main functional regions of 67LR are reported in Figure 1.

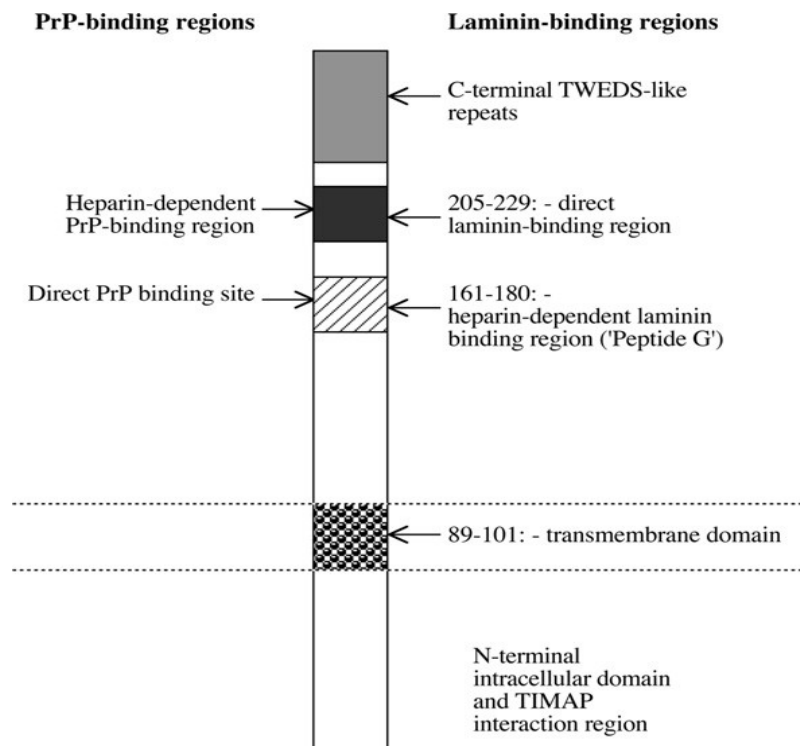


Fig. 1 Main functional regions and binding sites of 67LR.

67LR has three regions involved in laminin binding: the C-terminal TWEDS-like repeats, the stretch corresponding to aminoacids 205-229, and the so called peptide G (aa.161-180). The peptide G is also a direct binding site for prion protein (PrP), whereas region 205-229 is a heparin-dependent PrP-binding region.

1.2 67LR in tumor invasion and metastasis

67LR expression is increased in neoplastic cells as compared to their normal counterparts and directly correlates with an enhanced invasive and metastatic potential (Montuori 1996), mediated by high-affinity interactions between 67LR and laminin (Wewer 1987). Thus, 67LR overexpression is considered a molecular marker of metastatic aggressiveness in cancers of many

tissues, including breast, lung, ovary, prostate and also in leukaemia and lymphoma (Menard 1998; Montuori 1999; Chen 2002).

The role of 67LR in tumor progression is based on the adhesive properties of this receptor. Indeed, a key step in the metastatic process is the attachment of tumor cells to laminin, the major component of basement membranes. Interactions between tumor cells and basement membranes are mediated by specific membrane receptors, including 67LR, whose association with tumor aggressiveness has been convincingly demonstrated.

During intra-vasation and extra-vasation, cancer cells need to come into contact with and to degrade host basement membranes, before passing through. Proteolytic degradation of basement membrane components such as proteoglycans, collagen type IV, laminin-1, and laminin-5 occurs through the action of specific proteases secreted by tumor and stromal cells. This proteolytic cleavage removes physical barriers to cell migration and converts ECM components in substrates suitable for migration (Giannelli 1997). The invasive behavior of metastatic tumor cells correlates with the expression of many enzymes with hydrolytic activity as cysteine proteinases, cathepsin B, aspartic proteinases, cathepsin D, and serine proteinases, elastase (Yan et al 1998; Tetu et al 1999).

In addition to promoting tumor cell adhesion and migration, 67LR increases cancer cell invasion by up-regulating the expression and the activity of proteolytic enzymes able to degrade the extracellular matrix, such as membrane type 1 matrix metalloproteinase (MT1-MMP), stromelysin 3, cathepsin L, and the matrix metalloproteinase MMP-2 (Berno 2005).

An important role of 67LR in tumor progression has recently been described: mice inoculated with lung carcinoma cells expressing low levels of 67LR for the introduction of a specific antisense mRNA showed a prolonged survival (Satoh 1999). Therefore, new therapies aimed to inhibit 67LR were tested in mice (Koliakos 2002); moreover, vaccines anti-67LR have been tested successfully in the treatment of human metastatic renal cell carcinoma (Holtl 2002).

A recent study on HT1080 fibrosarcoma cells revealed that the use of strategies to inhibit the interaction of 67LR with its ligand may interfere with the invasive potential of these cells. Anti-67LR antibodies such as the single-chain antibody scFv iS18, its full-length version and the polysulfated glycans HM2602 and pentosan polysulfate (SP-54) significantly inhibited the invasion of HT1080 cells. HT1080 cells transfected with recombinant lentiviral plasmids expressing small interfering RNAs (siRNAs) directed against LRP mRNA revealed reduced levels of LRP, concomitant with a significantly reduced invasive behavior (Zuber 2008). A novel Sindbis/Lenti pseudotype vector carrying short-hairpin RNA (shRNA) designed against 67LR effectively reduced its expression and specifically targeted tumors in vivo. Treatment of tumor-bearing severe combined immunodeficient (SCID) mice with this pseudotype vector significantly inhibited tumor growth

(Scheiman 2010). Thus, 67LR can be used as a target in novel therapies for tumor reduction and elimination.

1.3 67LR crystal structure

Computational methods for drug design are based on the three dimensional structure of relevant cell targets. A high-resolution crystal structure of the majority of 37LRP, residues 1 through 220 (abbreviated LamR220) has been recently determined (PDB code 3BCH) (Jamieson 2008). LamR220 binds laminin with similar affinity as the full-length 67LR and inhibits Sindbis virus infection *in vitro*. Based on analysis of sequence conservation and of the crystal structures of human 37LRP and *Archaeoglobus fulgidus* S2 ribosomal protein, a laminin binding site has also been mapped (Jamieson 2010). The crystal structure of LamR is reported in Figure 2.

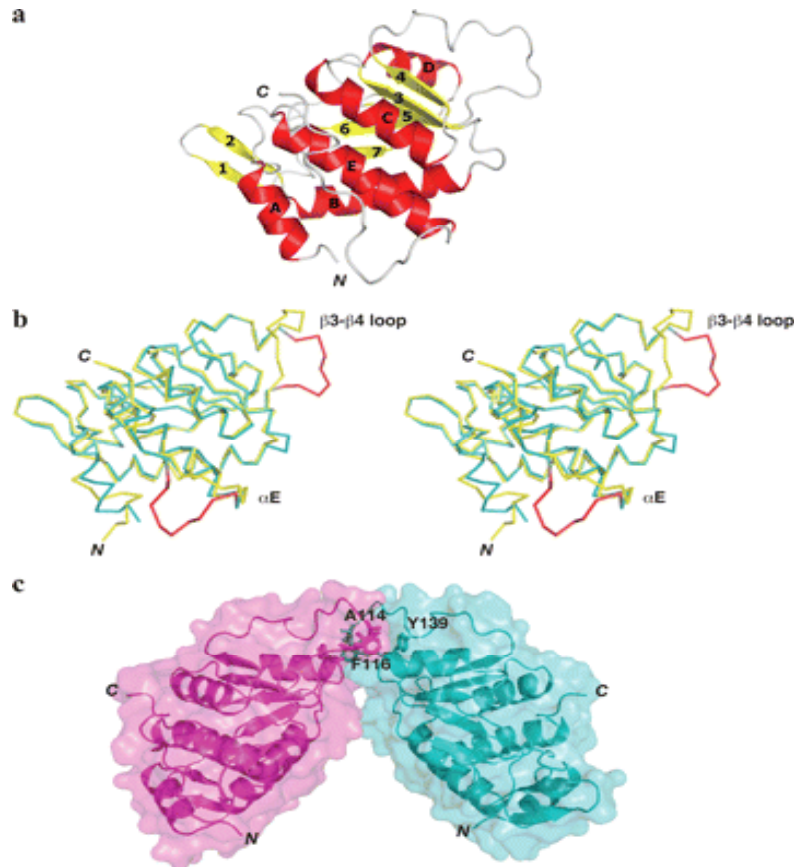


Fig. 2. Crystal structure of human LamR.

(a) Ribbon diagram of LamR220 with α helices colored red and β strands colored yellow. (b) Superimposition of LamR220 (cyan) and *A. fulgidus* S2p (1VI6) (yellow). Regions of divergence between the two structures are colored red in the 67LR structure (residues 111-118 and 188-196). (c) LamR220 dimer. One protomer is colored magenta and the other cyan. Residues in the dimer interface are labeled.

1.4 Phosphoprotein enriched in diabetes/phosphoprotein enriched in astrocytes-15 kDa (PED/PEA-15): structure and function

A yeast two-hybrid screening using phosphoprotein enriched in diabetes/phosphoprotein enriched in astrocytes-15 kDa (PED/PEA-15) as a bait identified 67LR as an interacting partner.

PED/PEA-15 is a 15-kDa ubiquitously expressed protein involved in the regulation of fundamental cellular functions, including apoptosis, proliferation, and glucose metabolism (Fiory 2009). PED/PEA-15 consists of a N-terminal nuclear export sequence, a death effector domain (DED), an extracellular regulated kinase (ERK) binding site, and two phosphorylation sites (Ser-104 and Ser-116) at the C terminus.

PED/PEA-15 lacks enzymatic function and serves mainly as a molecular adaptor. Since it contains a DED, PED/PEA-15 regulates apoptosis by competitively inhibiting the binding of DED-containing proteins to initiator caspases (Condorelli 1999; Kitsberg 1999).

Apart from its apoptosis-related effects, PEA-15 is a potent modulator of mitogen-activated protein kinase (MAPK) signaling cascades (Formstecher 2001). Unphosphorylated PED/PEA-15 binds ERK1/2 and prevents its translocation into the nucleus, thereby reducing the ERK1/2-mediated transcriptional activity and inhibiting cell proliferation (Callaway 2007; Renganathan 2005).

Moreover, PED/PEA-15 is an endogenous substrate for protein kinase C (PKC), calcium/calmodulin-dependent protein kinase II (CAM kinase II) and Akt. PKC phosphorylates PED/PEA-15 at Ser-104 (Kubes 1998) and CAM kinase II or Akt at Ser-116 (Trencia 2003; Formisano 2005). Phosphorylation of PED/PEA-15 at Serine-104 prevents ERK1/2-binding, thus allowing cell proliferation; phosphorylation at Serine-116 enhances the binding to Fas-associated protein with death domain (FADD) and caspase 8, resulting in inhibition of apoptosis (Kubes 1998; Trencia 2003).

A model for control of PED phosphorylation is depicted in Figure 3.

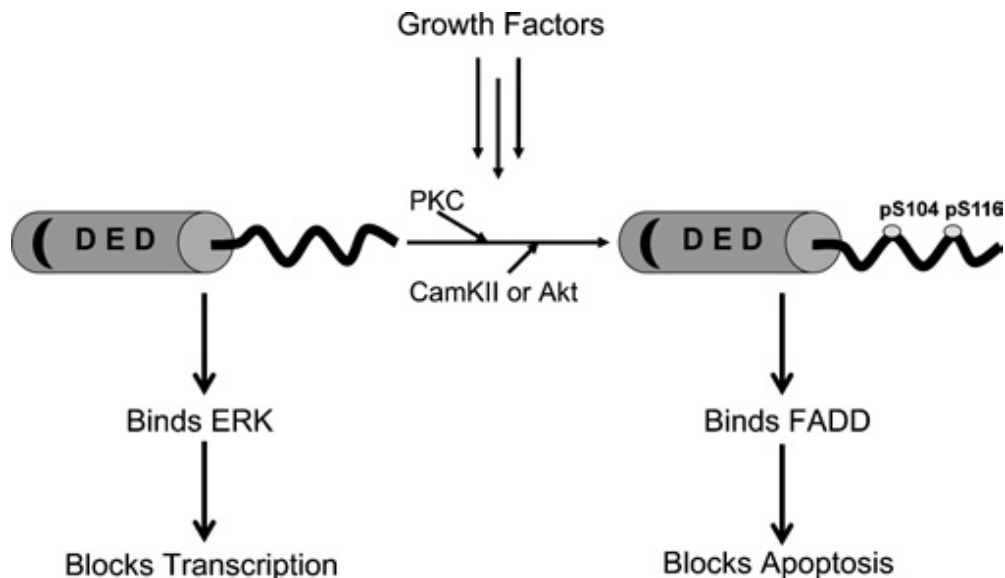


Fig. 3 Phosphorylation status of PEA-15 modulates its function in blocking ERK-mediated transcription or DISC-mediated apoptosis

A model for control of PEA-15 function by phosphorylation is depicted. Unphosphorylated PEA-15 binds ERK and prevents accumulation of active ERK in the nucleus, thus blocking transcription and slowing proliferation. Upon phosphorylation at Ser-104, PEA-15 cannot bind ERK. Upon phosphorylation at Ser-116, PEA-15 binds FADD and is thus recruited to the DISC in response to death receptor ligation. In this way, PEA-15 can integrate ERK- and FADD-dependent signalling pathways.

1.5 PED/PEA-15 in tumorigenesis and cancer progression

Because of its functional role in ERK signaling and apoptosis, increased PED/PEA-15 levels may affect tumorigenesis and cancer progression as well as sensitivity to anticancer agents. Overexpression of PED/PEA-15 in a transgenic mouse model increases the susceptibility to chemically induced skin cancer (Formisano 2005). Increased PEA-15 levels inhibit apoptosis in non small-cell lung cancer (Zanca 2008), B-cell chronic lymphocytic leukemia (Garofalo 2007), and thyroid cancer (Todaro 2006). In astrocytic tumors, PED/PEA-15 suppresses apoptosis (Hao 2001) and prevents glucose-induced cell death via the ERK pathway (Eckert 2008), suggesting that PED/PEA-15 promotes tumor cell survival in a poor microenvironment.

PED/PEA-15 also plays a role in the regulation of cell adhesion and migration; indeed, its binding to ERK1/2 regulates the affinity for fibronectin (FN) of integrin adhesion receptors (Chou 2003). In astrocytes, PEA-15 prevents cell migration through a PKC delta-dependent pathway (Renault-Mihara 2006). It has been recently reported that PED/PEA-15 interacts with Rac1 and its overexpression increases cell migration/invasion in human non-small cell lung cancer cells (Zanca

2010).

1.6 Structure-based drug design by “virtual screening”

High 67LR expression predicts for a more aggressive disease in several cancer types. Indeed, 67LR binding to the laminin of basement membranes is a prerequisite for tumor invasion and metastasis (Montuori 1996). These considerations prompted us to search for small molecules inhibiting 67LR by a computational methods.

The identification of a proper lead compound for a given molecular target is a critical step in drug discovery. To this end, computational tools are becoming increasingly important. Among them, “virtual screening” uses high-performance computing to analyze chemical databases and prioritize compounds for synthesis and assay.

There are two fundamental approaches for virtual screening, a ligand-based approach or a receptor-based approach. The ligand-based approach aims to identify molecules with physical and chemical similarities to known ligands that are likely to interact with the target. Receptor-based virtual screening (RBVS) aims to exploit the molecular recognition between a ligand and a target protein to select out chemical entities that bind strongly to the active sites of biologically relevant targets for which the three-dimensional structures are known or inferred.

RBVS starts with a 3-D structure of a target protein and a 3-D database of ligands and uses virtual filtering, followed by docking and scoring, to identify potential lead candidates. Docking and scoring algorithms generate subsets of a compound collection with a higher affinity against a target by predicting their binding mode (by docking) and affinity (by scoring), and retrieving those with the highest scores. The output of a docking-based screen is a set of 3-D models of the predicted binding mode of each compound against the receptor, together with a ranking that is a measure of the quality of fit. It thus represents the most detailed and relevant model for identifying a receptor-focused subset of ligands (Pierri 2010).

We conducted a receptor based virtual screening of a diversity library of small molecules, using the recently solved 67LR crystal structure.

In Figure 4 is depicted a model of “virtual screening” utilization.

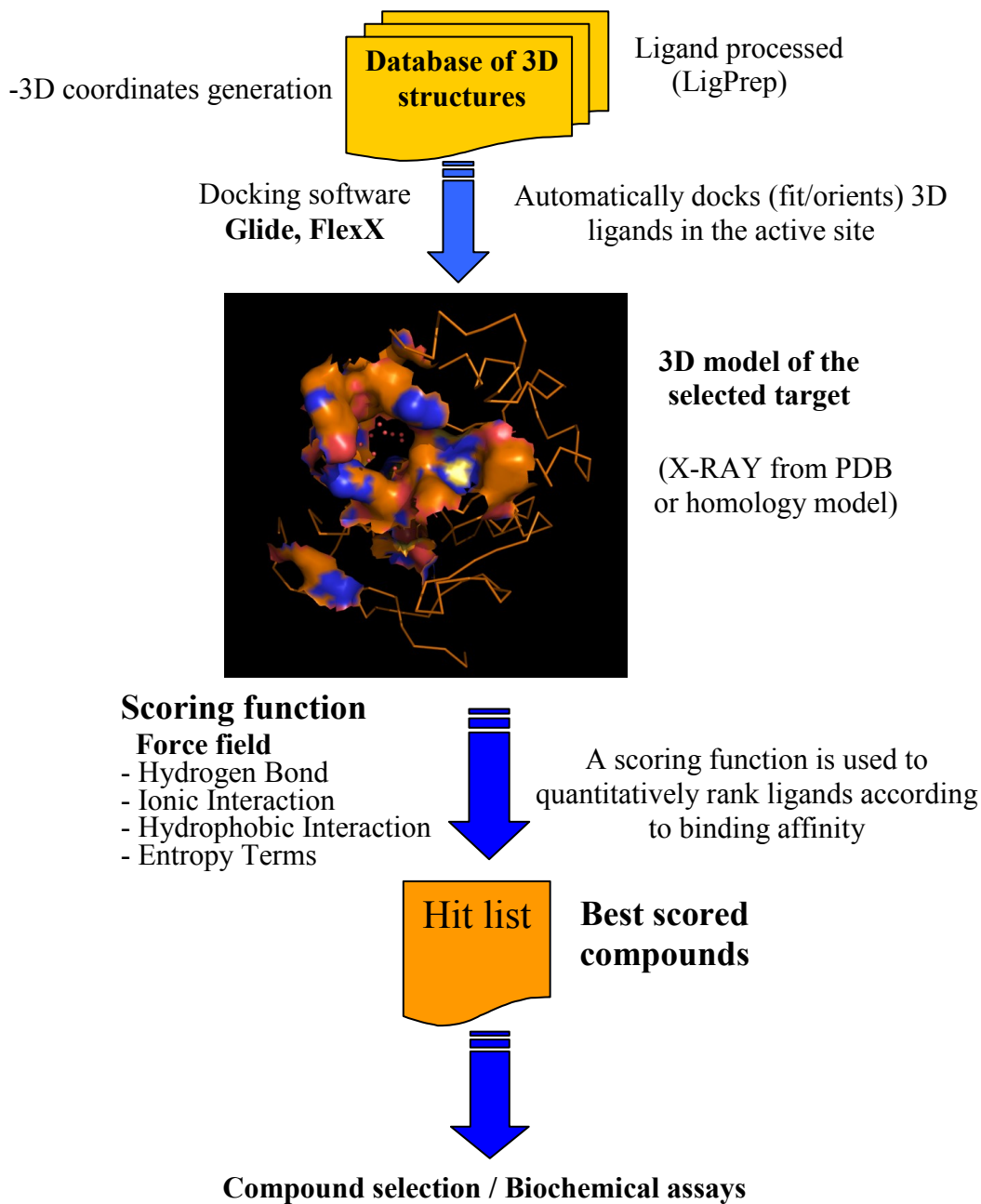


Fig.4 Virtual screening The structure-based virtual screening begins with the application of docking algorithms that *pose* small molecules in the active site of a selected target, determining whether a given conformation and orientation of a ligand fits it. Algorithms are complemented by *scoring functions* that are designed to predict the biological activity through the evaluation of interactions between compounds and potential targets.

2. AIMS OF THE STUDY

In this study, we aimed to confirm 67LR interaction with both overexpressed and endogenous PED/PEA-15 and to investigate the functional consequences of this interaction on cell adhesion, invasion/migration, proliferation and apoptosis.

Highly expressed 67LR regulates cancer aggressiveness and progression; indeed, high 67LR expression predicts for more aggressive disease in several types of cancer. These considerations prompted us to search for small molecules that might target 67LR on cancer cells.

Although siRNAs, single chain antibodies and Sinbis viral vectors able to disrupt 67LR interactions have been already described (Zuber 2008), we believe that small molecules with the same activity would be preferable; indeed, they are expected to have limited toxicity and to be orally available. Therefore, the identification of lead compounds with 67LR inhibitory activity could be a new promising tool for drug development in cancer therapy.

To this aim, we conducted a virtual screening of a diversity library of small molecules, using the recently solved 67LR crystal structure, with a focus on residues important for laminin binding. This screening identified many compounds that, in this study, were selected and characterized for their effects on cell adhesion, migration, invasion and proliferation in response to laminin.

3. MATERIALS AND METHODS

3.1 Materials

Media, sera, and antibiotics for cell culture and the Lipofectamine reagent were purchased from Invitrogen Ltd. (Paisley, United Kingdom). Mouse monoclonal anti-p-Akt and p-PKC antibodies and polyclonal anti-AKT antibody were from Cell Signaling Technology (Danvers, MA). Mouse monoclonal anti-p-ERK and PKC antibodies, rabbit polyclonal anti-ERK2 and CamKII antibodies were from Santa Cruz Biotechnology (Santa Cruz, CA). Rabbit polyclonal anti-p-CamKII antibody was from Upstate (Billerica, MA). Rabbit anti-67LR antibody, also recognizing 37LRP, was from Abcam (Cambridge, UK). Anti-His-tagged recombinant 37LRP antibody was made in our laboratory (Montuori 1999). Anti-caspase-3 antibody was from Calbiochem (San Diego, CA). Anti-PED/PEA-15 antibodies have been previously reported (Condorelli 1998). Antisera against phospho-Serine 104 and phospho-Serine 116 PED/PEA-15 were prepared in rabbits by PRIMM (Milan, Italy) and have been previously reported (Trencia 2003). Sodium dodecyl sulfate-polyacrylamide gel electrophoresis (SDS-PAGE) reagents were purchased from Bio-Rad (Richmond, VA). Western blotting and ECL reagents were from Amersham (Arlington Heights, IL). All other reagents were from Sigma (St. Louis, MO).

3.2 Transformation of Yeast Strains and β -Galactosidase Assay

Plasmid DNA transformations were performed using an high efficiency lithium acetate procedure (Gietz 1992). Cotransformants were propagated on Trp⁻, Leu⁻ plates, and potential interacting clones selected in Trp⁻, Leu⁻, His⁻, Ade⁻ media. After 4 days of incubation at 30 °C, positive clones were further tested for β -galactosidase activity by liquid culture assays using the substrate o-nitrophenyl- β -d-galactopyranoside as described by Miller et al. (Miller 1972). Clones of interest were analyzed by DNA sequencing and BLAST analysis.

3.3 Cell culture

The HEK-293 cell line was grown in DMEM medium supplemented with 10% heat-inactivated FCS. Transfected cells were grown in DMEM additioned with 10% FBS and with the below indicated antibiotics.

3.4 Transfection

PED/PEA-15 cDNA and 37LRP cDNAs were cloned in a pcDNA3 vector with resistance to Geneticin, and the resulting plasmids were named PED/PEA-15-pcDNA3 and 37LRP/pcDNA3. 5×10^6 cells, cultured overnight in 100 mm tissue culture dishes, were transfected with 10 μ g of PED/PEA-15-pcDNA3, 37LRP/pcDNA3 or with the empty vector pcDNA3 by 60 μ l of Lipofectamine for

5 h at 37°C (5% CO₂). Transfected cells, named PED-293, 67LR-293 and V-293, were selected by Geneticin at 1.5 mg/ml for 15 days, pooled and cultured in the presence of 0.5 mg/ml Geneticin.

3.5 Flow cytometric analysis of surface molecules

Flow cytometric analysis of cell surface molecules was performed as described previously (Montuori 1999). Briefly, cells were incubated for 2 h at 4°C with 20 µg/ml anti-67LR or isotype control antibodies. This step was followed by a second incubation for 1 h at 4°C with an anti-rabbit fluorescein-conjugated antibody. Finally, cells were washed and analyzed with a FACSCalibur Cytofluorimeter using Cell Quest software (Becton & Dickinson, San Fernando, CA). A total of 10⁴ events for each sample were acquired in all cytofluorimetric analyses.

3.6 Western blot

PED-293, LR-293 and V-293 cells were lysed in lysis buffer (50 mM HEPES [pH 7.5], 150 mM NaCl, 4 mM EDTA, 10 mM Na₄PO₇, 2 mM Na₃VO₄, 100 mM NaF, 10% glycerol, 1% Triton X-100, 1 mM phenylmethylsulfonyl fluoride, 100 mg of aprotinin/ml, 1 mM leupeptin) for 120 min at 4°C. Cell lysates were clarified at 5,000 x g for 15 min and the protein content was measured by a colorimetric assay. 50 µg of protein was electrophoresed on a 15% SDS-PAGE and transferred onto a PVDF membrane. The membrane was blocked with 5% non-fat dry milk, and probed with the primary and secondary antibodies; immunoreactive bands were detected by ECL according to the manufacturer's instructions.

For the detection of phosphorylated PED/PEA-15, ERK1/2, PKC, CAMKII and Akt, 5 x 10⁵ V-293 and PED-293 cells were plated onto 30 mm plates previously coated for 24 h with laminin (20µg/ml in PBS). After the indicated times, cells were washed with PBS, lysed and subjected to Western blot, as above described.

3.7 PED/PEA-15/67LR interaction

To investigate the interaction of PED/PEA-15 with 67LR, a 37LRP-His-tag fusion protein was generated. To this end, wild-type 37LRP cDNA (Montuori 1999) was cloned into the pTrcHis B expression vector (Invitrogen, San Diego CA) and expressed in TOP-10 bacteria (Invitrogen). His-tagged 37LRP (His-37LRP), was bound to nickel-NTA agarose beads, according to the procedures specified by Invitrogen. His-37LRP conjugated beads were washed and resuspended in 50 mmol/L Tris (pH 7.5)-0.1% Triton X-100. Lysates from PED/PEA-15-transfected 293 cells (500 µg) were incubated in the presence of 50 µl of agarose-bound His-37LRP (approximately 2 µg) for 2 h at 4°C. Beads were washed four times with 50 mmol/L Tris (pH 7.5)-0.1% Triton X-100 and then

resuspended in Laemmli buffer followed by boiling for 6 min and centrifugation at $25,000 \times g$ for 3 min. Supernatants were analyzed by SDS-PAGE and blotting with anti-PED-PEA-15 antibodies.

3.8 Coimmunoprecipitation

Cells were harvested and scraped into 1 ml of lysis buffer containing protease and phosphatase inhibitors. Total cell lysates were precleared with 20 μ l protein A-Sepharose beads (~50% slurry; Amersham Biosciences UK) at RT for 30 min. 5 μ g of anti-67LR, anti PED/PEA-15 or non-immune antibodies were added to 500 μ g of cleared lysate, and incubated for 2 h at 4°C. Then, 20 μ l of protein A-Sepharose beads were added and the lysates were incubated 30 min at RT. Immunoprecipitates were washed six times in lysis buffer and solubilized in 2 \times SDS-PAGE sample buffer. Western blotting with anti-67LR antibody was used to assay PED/PEA-15 co-immunoprecipitated 67LR in V-293 and PED-293 cells. Western blotting with anti-PED/PEA-15 antibody was used to detect 67LR co-immunoprecipitated PED/PEA-15 in U-373 cells. Separately, 25 μ g of total cell lysate was immunoblotted for 67LR and PED/PEA-15 to verify comparable expression in all samples.

3.9 Rac1 pull-down assay

V-293 and PED-293 cells were starved for 24 h and then plated on laminin-coated wells (10 μ g/ml) or BSA-coated wells, as a negative control, for the indicated times. After a quick wash with ice-cold PBS, cells were lysed with GST-Fish buffer (50mM Tris-HCl pH 7.4, 2mM MgCl₂, 1% NP-40, 10% glycerol, 100mM NaCl, 1mg/ml leupeptin, 1mg/ml pepstatin, 1mg/ml aprotinin, 1mM PMSF, and 2mM DTT). After 10 min at 4°C under agitation, cells were scraped and lysates were cleared by centrifugation in a precooled rotor. Five hundred micrograms of total protein extract was mixed with 10 μ g of GST-PAK-CRIB domain coupled to glutathione-sepharose beads (Upstate Biotechnology, Danvers, MA) and incubated 30 min at 4°C under agitation. Beads were then rinsed three times rapidly with 1ml of ice-cold GST-Fish buffer. The amounts of total Rac and Rac-GTP were estimated by immunoblot against Rac1 (Upstate Biotechnology).

3.10 Adhesion Assay

96-well flat-bottom microtiter plates were coated with 10 μ g/ml laminin (LM), vitronectin (VN), fibronectin (FN) or 1% heat-denatured BSA-PBS, as a negative control, and incubated overnight at 4°C. The plates were then blocked 1 h at room temperature with 1% heat-denatured BSA-PBS. Cells were harvested by 2 mM EDTA-PBS and resuspended in Ca²⁺/Mg²⁺-containing PBS. 10⁵ cells were plated in each coated well and incubated for 1 h at 37°C. Attached cells were fixed with 3% paraformaldehyde in PBS for 10 min and then incubated with 2%

methanol for 10 min. The cells were finally stained for 10 min with 0.5% crystal violet in 20% methanol. Stain was eluted by 0.1 M sodium citrate in 50% ethanol, pH 4.2, and the absorbance at 540 nm was measured by a spectrophotometer.

3.11 Cell proliferation assay

Cell proliferation was evaluated by a MTS (3-(4,5-dimethylthiazole-2-yl)-5-(3-carboxymethoxyphenyl)-2-(4-sulfophenyl)-2H-tetrazolium, inner salt) and PES (phenazine ethosulfate) assay (CellTiter 96 AQueous One Solution Reagent) provided by Promega (Madison, WI, USA). V-293, PED-293 and LR-293 cells were serum-starved overnight using DMEM 0.1% BSA, plated at 10^4 cells per well onto 96-well microtitre plates coated with 10 $\mu\text{g}/\text{ml}$ laminin (Costar 3599, Corning, New York, USA), in the same medium, and incubated for 1, 24, 48, 72 and 168 h at 37 °C, with 5% CO₂. 20 $\mu\text{l}/\text{well}$ of CellTiter 96 AQueous One Solution Reagent was added and, after 4 h incubation at 37 °C, the absorbance was determined by an ELISA reader (Bio-Rad, Hercules, California, USA) at a wavelength of 490 nm.

3.12 Cell apoptosis assay

V-293 and PED-293 cells were serum-starved overnight using DMEM 0.1% BSA. 10^6 cells were harvested by 2mM EDTA-PBS and plated in 100mm dishes precoated with 10 $\mu\text{g}/\text{ml}$ LM. After 24, 48 and 72 h at 37° C, 5% CO₂, cells were lysed and apoptosis was analyzed using the ApoAlert Caspase-3 Colorimetric Assay Kit (Clontech, CA, USA) that measures the proteolytic cleavage of the chromophore p-nitroanilide (pNA) by caspase-3. Some experiments were performed in the presence or in the absence of the anti-67LR antibody (10 $\mu\text{g}/\text{ml}$).

3.13 Cell Migration Assay

Cell migration assays were performed in Boyden chambers using 8 μm pore size PVPF polycarbonate filters coated with 5 $\mu\text{g}/\text{ml}$ FN, as an adhesion substrate. V-293, PED-293 and LR-293 cells (2×10^5) were plated in the upper chamber in serum-free medium. 50 $\mu\text{g}/\text{ml}$ laminin or serum free medium was added in the lower chamber. The cells were allowed to migrate for 6 h at 37°C, 5% CO₂. The cells on the lower surface of the filter were then fixed in ethanol, stained with hematoxylin, and counted at 200x magnification (10 random fields/filter). In a separate set of experiments, transfected cells were preincubated for 1 h at room temperature with 20 $\mu\text{g}/\text{ml}$ of a polyclonal antibody directed to 67LR and with non immune antibodies, as a negative control, or with 20 μM NSC47924 or DMSO, as a negative control.

3.14 Invasion assay

The upper chamber of the Boyden apparatus was filled with 100 μl of BD

Matrigel™ (BD Biosciences, San Jose, CA). BD Matrigel™ was diluted to 1mg/ml in serum free culture medium and put into the top of the filter. Then it was incubated for 4 h for gelling. V-293, PED-293 and LR-293 cells were counted, treated as indicated above and allowed to invade toward 10% FCS, or medium alone, as a negative control. Invaded cells were measured as % over control. In a separate set of experiments, transfected cells were preincubated for 1 h at room temperature with 20 µg/ml of anti-67LR polyclonal antibodies and non immune antibodies, as a negative control, or with 20 µM NSC47924 and DMSO, as a negative control.

3.15 Statistical analysis

Differences between groups were evaluated by the Student's t test using PRISM software (GraphPad, San Diego, CA). $P \leq 0.05$ was considered statistically significant.

4. RESULTS

4.1 Isolation and identification of 37 kDa laminin receptor precursor (37LRP) as a novel PED/PEA-15 interacting protein

To search for proteins specifically interacting with PED/PEA-15, a yeast two-hybrid system was established using the full-length ped/pea-15 gene (pG-BKT7-ped/pea-15) as bait to screen a human HeLa library (Clontech). Upon HIS3 selection, 45 β -galactosidase positive cDNA clones were detected. Based upon sequence analysis and BLAST searching, several clones were shown to match the 37LRP sequence (Rao 1989).

4.2 67LR interacts with PED/PEA-15 *in vitro* as well as in mammalian cells

To verify the interaction of 67LR with PED/PEA-15, pull-down assays were performed with His-tag-fused recombinant 37LRP on lysates of 293 cells stably transfected with PED/PEA-15 (PED-293 cells) (Fig.5A). Recombinant 37LRP bound PED/PEA-15 in PED-293 cell extracts (Fig. 5B). No pull-down was detectable using His-tag bound agarose, indicating that 37LRP specifically binds PED/PEA-15 *in vitro*.

Dimerization of 37LRP (Rao 1989; Landowski 1995) generates the mature form of the receptor, the 67 kDa laminin receptor (67LR). 37LRP is localized mostly in the cytoplasm, acting as a precursor for 67LR, but also as a ribosomal protein and in the nucleus, where it interacts with histones (Montuori 1996). 67LR is localized in the plasma membrane, where it binds laminin (LM) with high affinity, thus playing a crucial role in tumor invasion and metastasis (Rao 1989; Landowski 1995; Castronovo 1991; Kazmin 2000; Montuori 1996).

We sought to define the receptor form interacting with PED/PEA-15 by coimmunoprecipitation experiments in PED-293 cells, stably transfected with PED/PEA-15 cDNA and endogenously expressing 37LRP and 67LR (Fig.5C). Precipitation of lysates from PED-293 cells with anti-PED/PEA-15 antibodies followed by blotting with antibodies able to recognize both 37LRP and 67LR revealed co-precipitation of 67LR, indicating that PED/PEA-15 interacts with the mature membrane-bound form of the receptor (Fig.5C). Moreover, coimmunoprecipitation experiments in U-373 glioblastoma cells, endogenously expressing both PED/PEA-15 and 67LR (not shown), with anti-67LR antibodies followed by blotting with anti-PED/PEA-15 antibodies revealed co-precipitation (Fig.5D).

Therefore, endogenous and overexpressed PED/PEA-15 specifically interacts with the mature membrane bound 67LR.

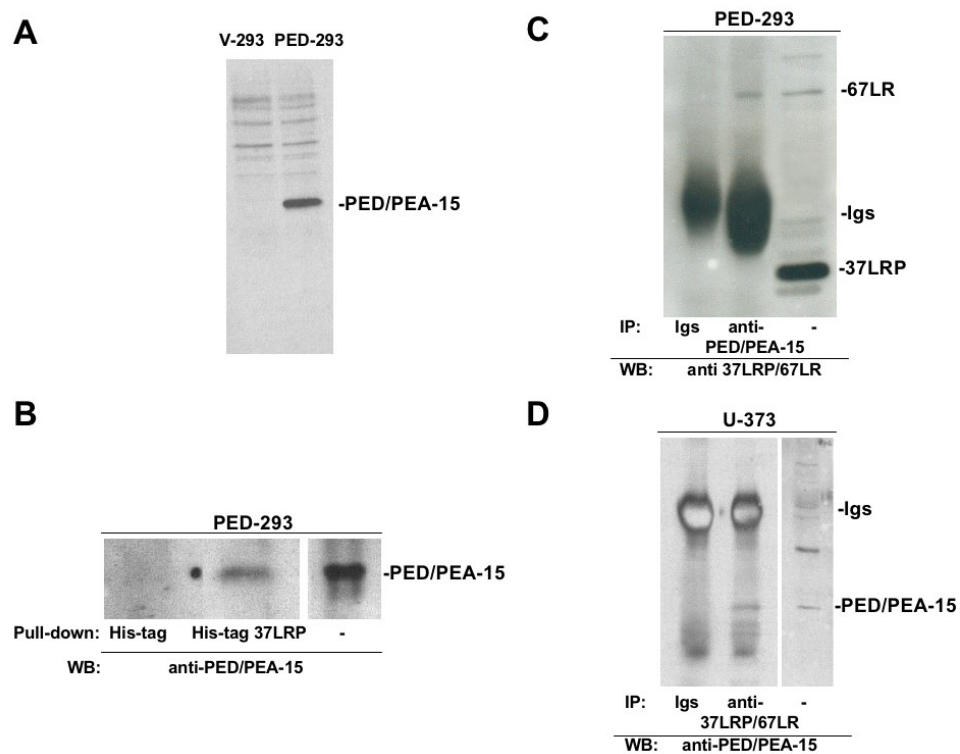


Fig.5. PED/PEA-15 interacts with 67LR.

A: HEK-293 cells were transfected with PED/PEA-15 cDNA (PED-293) or with the empty vector (V-293). Transfected cells were lysed and 50 μ g of proteins were analyzed by Western blot with PED/PEA-15-specific antibodies. PED-293 cells express PED/PEA-15.

B: Lysates from PED-293 cells were incubated with agarose-bound recombinant His-tagged 37 kDa laminin receptor precursor (His-tag 37LRP) or with agarose bound His-tag (His-tag), as a negative control. His-tag 37LRP conjugated beads were washed, resuspended in Laemmli buffer, boiled and supernatants were analyzed by SDS-PAGE and blotting with anti-PED/PEA-15 antibodies. Separately 50 μ g of total PED-293 lysate was immunoblotted (input). Recombinant 37LRP binds PED/PEA-15.

C: PED-293 cell lysates were incubated with 5 μ g of a polyclonal anti-PED/PEA-15 antibody or with non-immune immunoglobulins (Igs). The lysates were then immunoprecipitated with protein A Sepharose beads, washed and solubilized in Laemmli sample buffer. Western blotting with a polyclonal antibody, able to recognize both the 37LRP and the mature 67LR (anti-37LRP/67LR), was used to detect co-immunoprecipitated 67LR. Separately, 50 μ g of total cell lysate was immunoblotted for 37LRP/67LR (input). In PED/PEA-15 overexpressing cells, PED/PEA-15 is exclusively associated to the mature membrane-bound form of 67LR.

D: U-373 cell lysates were incubated with 5 μ g of a polyclonal anti-67LR antibody. The lysates were then immunoprecipitated with protein A Sepharose beads, washed and solubilized in Laemmli sample buffer. Western blotting with a polyclonal anti-PED/PEA-15 antibody was used to detect co-immunoprecipitated PED/PEA-15. Separately, 50 μ g of total cell lysate was immunoblotted for PED/PEA-15 (input). In U-373 glioblastoma cells, endogenously expressed PED/PEA-15 is associated to 67LR

4.3 PED/PEA-15 overexpression increases 67LR-mediated cell adhesion to laminin

PED/PEA-15 is overexpressed in different human tumors, including breast and lung cancer, in which it determines refractoriness to anticancer therapy and resistance to apoptosis (Eckert 2008; Chou 2003; Renault-Mihara 2006; Zanca 2010). Therefore, we investigated the functional effects of PED/PEA-15 interaction with 67LR in PED/PEA-15 overexpressing cells.

First, we sought to investigate whether PED/PEA-15 overexpression could influence 67LR-mediated cell functions, namely, cell adhesion and migration to LM. Thus, V-293 and PED-293 cell adhesion to LM, fibronectin (FN) and vitronectin (VN) were evaluated. PED-293 cell adhesion to LM was significantly increased, as compared to V-293; conversely, PED-293 cell adhesion to VN and FN was not affected (Fig.6A). Moreover, the increase in PED-293 cell adhesion to LM was completely abrogated by cell pre-treatment with anti-67LR antibodies (Fig. 6B).

Increased PED-293 cell adhesion to LM was not due to 67LR overexpression; indeed, V-293 and 293-PED cells showed comparable levels of 67LR expression by cytofluorimetric analysis (Fig. 6C).

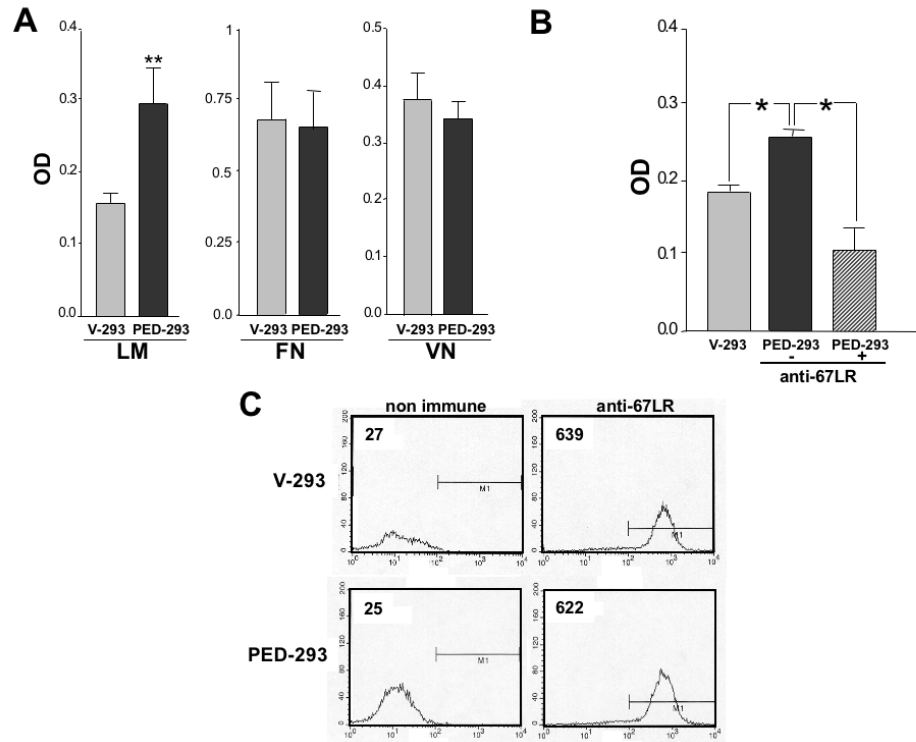


Figure 6: PED/PEA-15 overexpression increases 67LR-mediated cell adhesion to laminin.

A: V-293 (□) and PED-293 (■) cells were incubated for 1 hour on laminin (LM), vitronectin (VN), fibronectin (FN) or 1% heat-denatured BSA coated wells. The attached cells were fixed, permeabilized and stained with crystal violet. The stain was eluted and the absorbance at 540 nm (OD) was measured by a spectrophotometer. Cell adherence to BSA was subtracted from the reported values, representing the mean±S.D. of six experiments performed in triplicate. (*) $p \leq 0.05$, as determined by the Student's *t* test. PED-293 cell adhesion to LM was significantly increased, as compared to V-293; PED-293 cell adhesion to VN and FN was not affected.

B: V-293 (□) and PED-293 (■) cells were plated on LM-coated wells in the presence of 20 $\mu\text{g/ml}$ of nonimmune immunoglobulins (-) or anti-67LR polyclonal antibodies (▣). The attached cells were fixed and stained with crystal violet. The stain was eluted, and the absorbance at 540 nm was measured by a spectrophotometer. The values represent the means±S.D. of three experiments performed in triplicate. (*) $p \leq 0.05$, as determined by the Student's *t* test. Increased PED-293 cell adhesion to LM was abrogated by anti-67LR antibodies.

C: Flow cytometric analysis of cell surface 67LR expression was evaluated by incubating V-293 and PED-293 cells with a polyclonal anti-67LR antibody or an isotype control. Fluorescence intensity values are reported. Increased PED-293 cell adhesion to LM was not due to increased 67LR expression; V-293 and 293-PED cells showed comparable levels of 67LR expression.

4.4 PED and 67LR interaction increases cell migration/invasion toward laminin and affects ECM signaling

PED/PEA-15 overexpression also resulted in increased cell migration to LM and matrigel invasion. Moreover, PED-293 cell pretreatment with an anti-

67LR antibody was able to inhibit both cell migration to LM and matrigel invasion (Fig 7A, B).

Therefore, PED/PEA-15 overexpression increases cell adhesion and migration to LM, through its physical interaction with 67LR. In order to study the downstream effects of PED/PEA-15 and 67LR interaction, we investigated ERK 1/2 pathway. Indeed, one of the most important effects of the activation of ERK1/2 pathway is the regulation of cell migration and invasion (Reddy 2003). PED/PEA-15 activates ERK/MAP Kinase through a Ras-dependent pathway (Ramos 2000). Moreover, Rac1, a member of mammalian Rho GTPase protein family, has been recently identified as PED/PEA-15-interacting protein (Zanca 2010). In a non small cell lung (NSCL) cancer cell line, PED/PEA-15 overexpression promotes Rac1 activation in response to growth factor stimulation; in turn, active Rac1 increases ERK 1/2 phosphorylation (Zanca 2010; Eblen 2002).

To determine the effect of PED/PEA-15 and 67LR interaction on ERK 1/2 and Rac1 activation after cell adhesion to LM, we plated control V-293 and PED-293 cells on LM and then evaluated ERK 1/2 phosphorylation by Western blot analysis and Rac1 activation by pull-down assay.

PED/PEA-15 overexpression was able to activate ERK 1/2, as compared to control V-293 cells (Fig.7C). Interestingly, cell adhesion to LM also promoted Rac1 activation in PED/PEA-15 overexpressing cells, as compared to vector transfected cells (Fig. 7D).

These results show for the first time that PED/PEA-15 overexpression promotes cell migration and invasion through LM, the major component of basal membranes. This effect is mediated by PED/PEA-15 interaction with 67LR, leading to increased cell adhesion to LM, Rac1 activation and ERK1/2 phosphorylation.

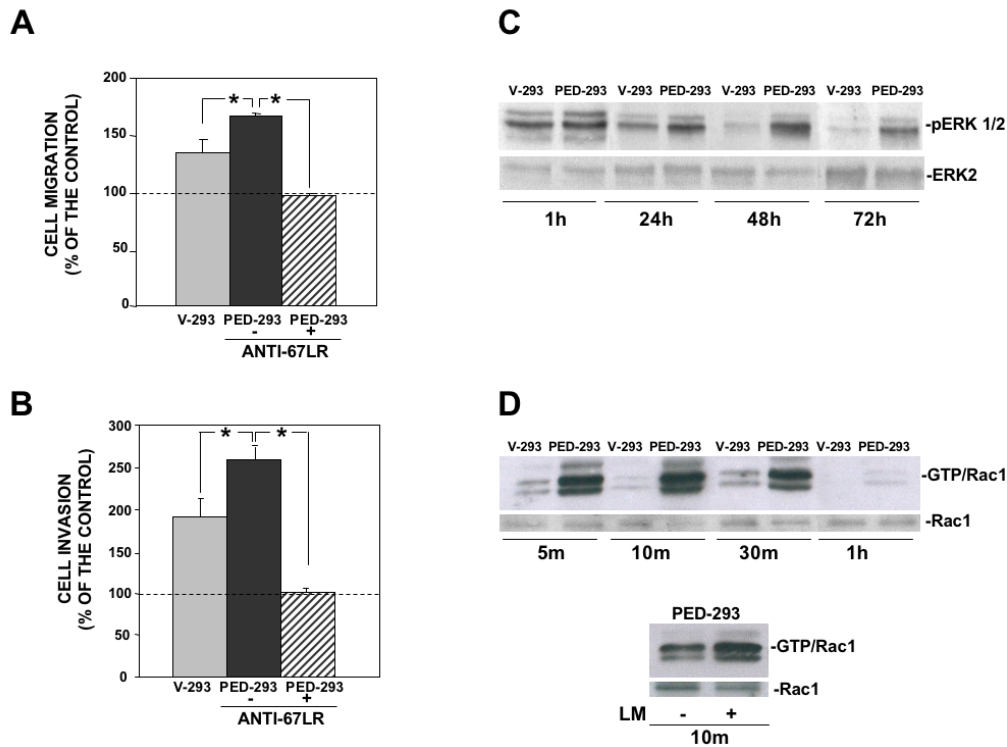


Figure 7: PED/PEA-15 overexpression increases 67LR-mediated migration to LM and matrigel invasion by activating ERK 1/2 and Rac1.

A: V-293 (□) and PED-293 (■) cells were pre-incubated with nonimmune Ig or a polyclonal anti-67LR antibody (▣), plated in Boyden chambers and allowed to migrate toward 50 μg/ml LM on filters coated with 10 μg/ml FN. The values are the mean±SD of three experiments performed in triplicate. (*) p<0.05, as determined by the Student's *t* test.

B: V-293 (□) and PED-293 (■) cells were pre-incubated with nonimmune Igs (-) or a polyclonal anti-67LR antibody (▣), plated in Boyden chambers and allowed to invade matrigel^{PM}. The values are the mean±SD of three experiments performed in triplicate. (*) p<0.05, as determined by the Student's *t* test. PED overexpression increased cell migration to LM and matrigel invasion; pretreatment with anti-67LR antibody inhibited both cell migration and invasion.

C: V-293 and PED-293 cells were serum-starved and plated on uncoated or LM coated wells. The cells were harvested at the indicated times and lysed for Western blot analysis with anti-phospho-ERKs and anti-ERK 2 (as a loading control) antibodies.

D: V-293 and PED-293 cells were serum starved and then plated on uncoated or LM-coated wells for the indicated times. Rac1-GTP pull down assay was performed as described in Materials and Methods Section. The amounts of total Rac1 and Rac1-GTP were estimated by immunoblotting with Rac1. PED-293 cell adhesion to LM activated Rac1.

PED/PEA-15 overexpression affected ECM signaling in 67LR expressing cells.

4.5 Cell adhesion to LM allows cell proliferation in PED/PEA-15 overexpressing cells by modulating PED/PEA-15 phosphorylation status

We also investigated whether 67LR interaction with PED/PEA-15 could result in a modulation of PED/PEA-15 cellular functions. To this aim, we analyzed PED-293 and V-293 cell proliferation after adhesion to LM (Fig.8A). LM induced

a strong proliferative response in V-293 cells whereas PED/PEA-5 overexpression strongly inhibited cell proliferation, as reported (Zanca 2010; Glading 2007). However, after 24h, PED-293 cells recovered their proliferative capacity, albeit significantly slower than control cell, reaching them at 168h. V-293 and PED-293 cell number, after adhesion to LM, followed the same pattern (Fig.8B).

PED/PEA-15 can bind and retain into cytosol extracellular-regulated kinases 1/2 (ERK 1/2), independently of their phosphorylation status, thus avoiding cell proliferation. On the other hand, PED/PEA-15 phosphorylation inhibits the interaction with ERK1/2 and abrogates the ability to block ERK1/2 transcriptional activities, thus enabling the proliferation of cells expressing high levels of PED/PEA-15 (Krueger 2005).

Therefore, we asked whether 67LR-mediated cell adhesion to LM could alter PED/PEA-15 phosphorylation status, particularly after 24h, when PED-293 cells started to recover their proliferative capacity. To this aim, we analyzed PED/PEA-15 phosphorylation status after PED-293 cell adhesion to LM or BSA, as a negative control (Fig.8C). After 1h of cell adhesion to LM, PED/PEA-15 became phosphorylated both in Ser-104 and in Ser-116; at 24h phosphorylation reached the maximum, and then remained unchanged up to 72h (not shown).

Therefore, 67LR interaction with PED/PEA-15 increases cell adhesion and migration/invasion to LM and, in turn, stimulates PED/PEA-15 phosphorylation, thus enabling cell proliferation in response to LM.

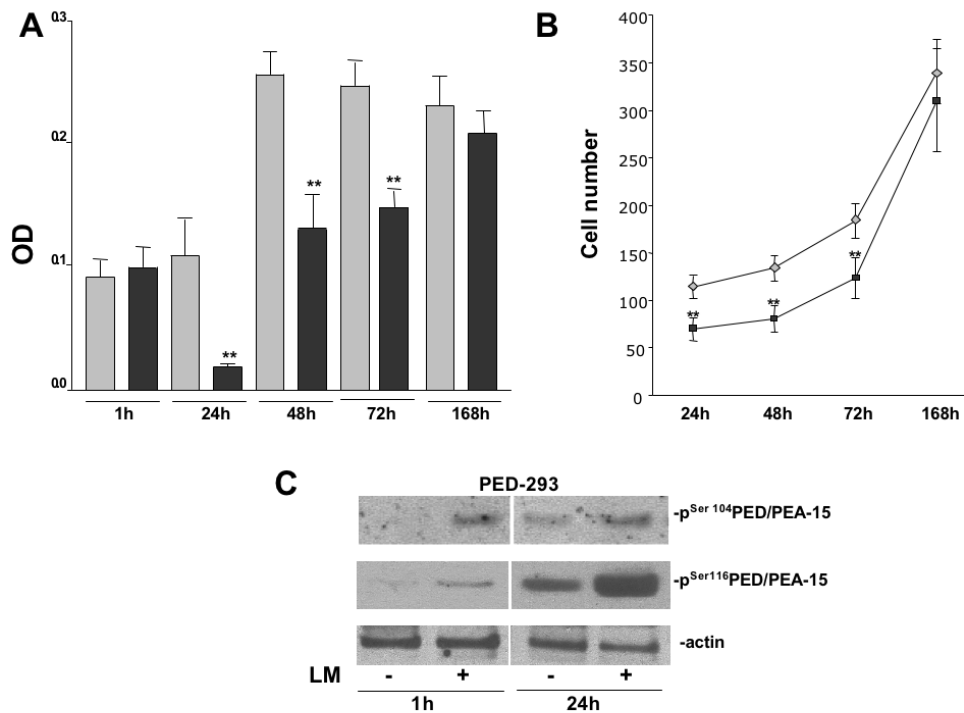


Figure 8: 67LR interaction with PED/PEA-15 modulates LM-mediated cell proliferation and PED/PEA-15 phosphorylation status.

A: V-293 (□) and PED-293 (■) cell proliferation were evaluated by a MTS assay after adhesion to LM-coated wells. At the indicated times 20 μ l/well of reagent was added and the absorbance (OD) was determined at a wavelength of 490 nm. The values are the mean \pm SD of three experiments performed in triplicate. (*) $p < 0.05$, as determined by the Student's *t* test. After 24 hours of adhesion to LM, PED-293 cells recovered their proliferative capacity, reaching V-293 cells at 168h.

B: V-293 (◇) and PED-293 (■) cell number was evaluated after adhesion to LM, at the indicated times. The values are the mean \pm SD of three experiments performed in triplicate. (*) $p < 0.05$, as determined by the Student's *t* test.

C: PED-293 cells were serum-starved and plated on uncoated or LM coated wells. The cells were harvested at the indicated times and lysed for Western blot analysis with anti-phospho Ser-104 PED/PEA-15 and anti-phospho Ser-116 PED/PEA-15 antibodies; anti-actin antibodies were used as a loading control. 67LR-mediated cell adhesion to LM induced PED/PEA-15 phosphorylation both in Ser-104 and Ser-116.

4.6 Cell adhesion to LM also inhibits apoptosis in PED/PEA-15 overexpressing cells

When phosphorylated in Ser-104 and Ser-116, PED/PEA-15 is recruited to the DISC and inhibits the apoptotic process (Renganathan 2005). Therefore, we asked whether LM-induced PED/PEA-15 phosphorylation could alter the apoptotic response to serum deprivation in PED-293 cells. To this aim, V-293 and PED-293 cells were plated on LM in the absence of serum and apoptosis was evaluated at

different times by ELISA assay. No apoptosis could be detected after 24h of serum deprivation; at 48h, V-293 cells underwent apoptosis whereas PED-293 cells showed a significant resistance (Fig. 9A). Noteworthy, cell-treatment with anti-67LR antibodies restored PED-293 cell sensitivity to serum-deprivation induced apoptosis. After 48h of PED-293 cell adhesion to LM, resistance to apoptosis was also evidenced by the strong reduction of caspase 3 activation in respect to V-293 cells (Fig. 9B).

Therefore, 67LR-dependent binding to LM, through PED/PEA15 phosphorylation, can restore cell proliferation and inhibit the apoptotic process.

4.7 Cell adhesion to laminin regulates PED-PEA-15 phosphorylation by activating protein Kinase C and calcium/calmodulin-dependent protein Kinase II

We demonstrated that increased 67LR-mediated cell adhesion to LM in PED-PEA-15 overexpressing cells promotes cell proliferation and resistance to apoptosis by determining PED-PEA-15 phosphorylation both in Ser-104 and Serine-116.

PED/PEA-15 is an endogenous substrate for protein kinase C (PKC), calcium/calmodulin-dependent protein kinase II (CAM kinase II), and Akt. In particular, PKC phosphorylates PED/PEA-15 at Ser-104 and CAM kinase II or Akt at Ser-116. Phosphorylation of PEA-15 at Serine-104 prevents ERK1/2-binding and phosphorylation at Serine-116 enhances the binding to Fas-associated protein with death domain (FADD) and caspase 8, resulting in cell proliferation and inhibition of apoptosis (Renganathan 2005; Kubes 1998; Trencia 2003).

Therefore, we investigated whether increased cell adhesion to LM could increase PKC, CAMKII or Akt activation in PED-293 cells as compared to vector transfected V-293 cells. After plating PED-293 cells on LM coated wells, PED/PEA-15, PKC, CAMKII and Akt phosphorylation status was evaluated by Western blot analysis with phosphospecific antibodies (Fig.9C). Akt was not activated whereas CAMKII was phosphorylated after 1 h, 24h, and up to 72h (not shown); thus, after cell adhesion to LM, Ser-116 could be phosphorylated by CAMKII. PKC was transiently activated at 1 h and could directly phosphorylate Ser-104.

Therefore, increased 67LR mediated cell adhesion to LM in PED/PEA-15 overexpressing cells stimulate a signal transduction pathway that, through PKC and CAMKII activation, determines PED/PEA-15 phosphorylation in both Ser-104 and Ser-116. PED/PEA-15 phosphorylation enables cell proliferation and resistance to apoptosis.

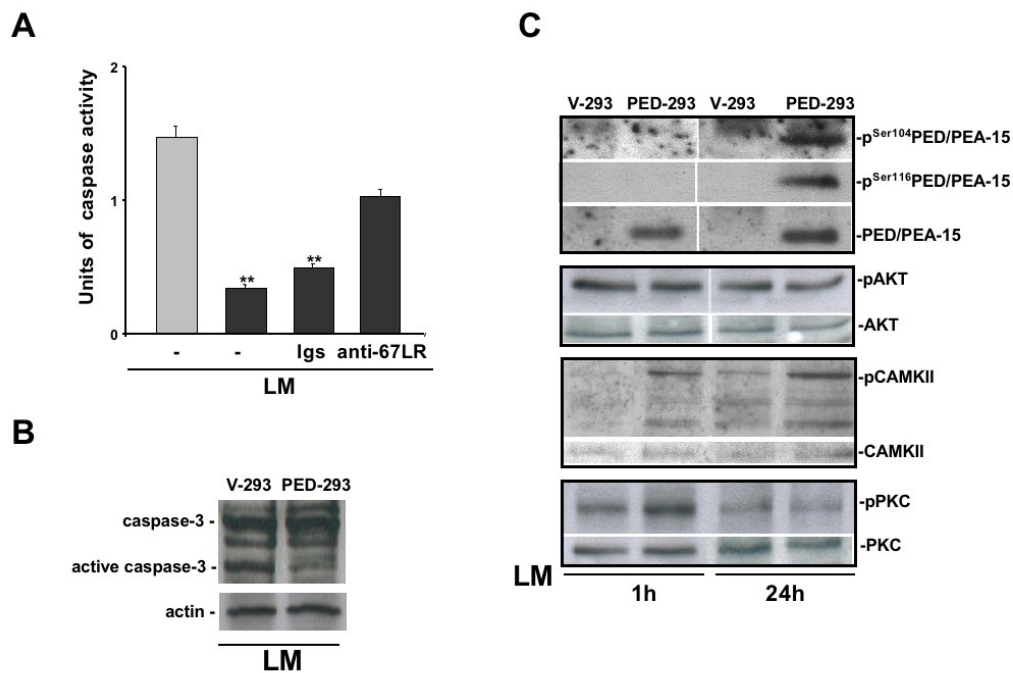


Figure 9: 67LR-mediated cell adhesion to LM inhibits apoptosis in PED/PEA-15 overexpressing cells and activates a signal transduction pathway responsible for PED/PEA-15 phosphorylation.

A: V-293 (□) and PED-293 (■) cells were plated on LM in the absence of serum and apoptosis was evaluated at different times by ELISA assay in the presence of medium alone (-), 20 µg/ml of nonimmune immunoglobulins (Igs) or anti-67LR polyclonal antibodies. The values are the mean±SD of three experiments performed in triplicate. (*) $p \leq 0.05$, as determined by the Student's *t* test. At 48h, PED-293 cells showed a significant resistance to apoptosis; anti-67LR antibodies restored PED-293 cell sensitivity to serum-deprivation induced apoptosis.

B: V-293 and PED-293 cells were plated on LM for 48 h in the absence of serum and apoptosis was evaluated by Western blotting with anti-caspase 3 antibodies. A strong reduction of caspase 3 activation was observed in PED-293 cells as compared to V-293 cells.

C: V-293 and PED-293 cells were serum-starved and plated on LM coated wells. The cells were harvested at the indicated times and lysed for Western blot analysis with anti-phospho^{Ser104} PED/PEA-15, anti-phospho^{Ser116} PED/PEA-15, anti-phospho-CAMKII, anti-phospho-Akt and anti-phospho-PKC antibodies; anti-PED/PEA-15, CAMKII, Akt and PKC antibodies were used as a loading control.

4.8 Virtual screening of a diversity library of small molecules on 67LR

The in silico screening of a library of chemical compounds for their potential to disrupt 67LR/LM interactions is the culmination of a long effort to find ways to inhibit 67LR-mediated cancer cell invasion and metastasis. It was made possible by the identification and characterization of a specific LM binding sequence on 67LR (Taraboletti 1993) and the recently published crystal structure of 67LR (Jamieson 2008).

A diversity library of about 13,000 small molecules was screened using Autodock

(v 3.05) for possible binders to 67LR and to the specific site on 67LR that binds LM. The input describing the protein was prepared with the program Autodock Tools (ADT); it involved adding charges and non-bonded parameters to the protein structure file and orienting the protein to minimize the enclosing rectangle using an in-house program, Simulaid. The screening and the filtering of the docked poses were driven, respectively, by a script and a program (Dockres). Of the top-scoring molecules that docked on 67LR, 43 showed preferential docking on the sequence consisting of residues 161-180 and those were further tested in a cell-based assay.

4.9 37LRP cDNA transfection in HEK-293 cells results in cell surface expression of the mature receptor and increased cell adhesion to laminin

To obtain a cell system expressing high levels of 67LR, HEK-293 cells were transfected with a cDNA encoding the 37LRP fused at the C-terminal with a tag derived from a phage T7 sequence and a poly-histidine stretch (37LRP/His-tag), these cells were named LR-293. As a negative control, HEK-293 cells were transfected with the empty vector pcDNA3 and named V-293.

37LRP/His-tag expression in transfected cells was demonstrated by Western blot analysis with both a specific anti-37LRP antibody, made in our laboratory against the His-tagged recombinant 37LRP, and an anti-T7 tag antibody (Fig. 10A).

To verify that transfected 37LRP was correctly processed and expressed at the cell surface, flow cytometry analysis was performed on live V-293 and LR-293 cells with the anti-67LR antibody (Abcam). LR-293 cells showed increased 67LR surface expression in respect to V-293 cells (Fig. 10B).

Moreover, the receptor expressed on LR-293 cell surface was functionally active; indeed, LR-293 cell adhesion to LM was significantly increased, as compared to V-293 cells, and such increase was completely abrogated by cell pre-treatment with anti-67LR antibodies (Fig. 10C).

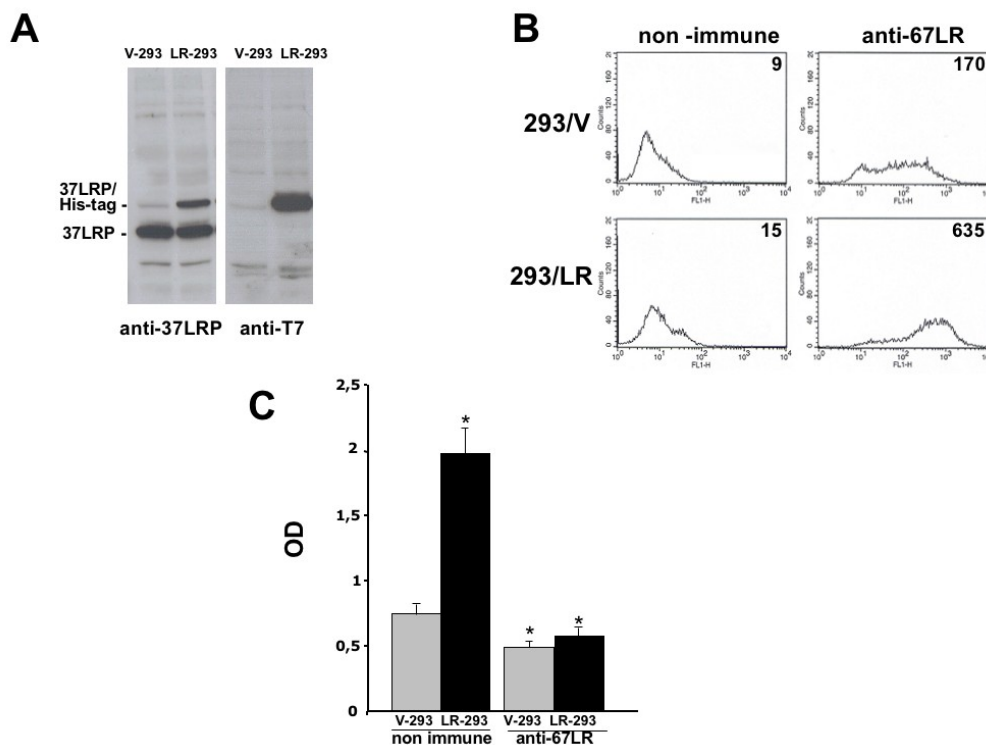


Figure 10. 37LRP cDNA transfection in HEK-293 cells results in cell surface expression of the mature receptor and increased cell adhesion to laminin.

A: HEK-293 cells were transfected with a cDNA coding for 37LRP fused at the C-terminal with a tag derived from a phage T7 sequence and a poly-histidine stretch (37LRP/His-tag), and named LR-293, or with the empty vector, V-293. Transfected cells were lysed and 50 µg of proteins were analyzed by Western blot with anti-His tagged recombinant 37LRP and T7 specific antibodies.

B: Flow cytometric analysis of cell surface 67LR expression was evaluated by incubating V-293 and LR-293 cells with a polyclonal anti-67LR antibody or an isotype control. Fluorescence intensity values are reported.

C: V-293 (□) and LR-293 (■) cells were plated on LM-coated wells in the presence of 20 µg/ml non immune immunoglobulins or anti-67LR polyclonal antibodies. The attached cells were fixed and stained with crystal violet. The stain was eluted, and the absorbance at 540 nm was measured by a spectrophotometer. The values represent the means±S.D. of three experiments performed in triplicate. (*) p≤0.05, as determined by the Student's *t* test.

4.10 LR-293 cell adhesion to laminin is inhibited by molecules selected by Virtual Screening

In order to identify an inhibitor of 67LR interaction with LM, in vitro assays of LR-293 cell adhesion to LM were performed in the presence of the molecules selected by virtual screening.

LR-293 cells were plated in LM-coated wells in the presence of the selected molecules, dissolved in DMSO and added at a concentration of 2×10^{-5} M, corresponding to 10,000-fold the affinity constant of 67LR for LM (2×10^{-9} M);

DMSO was used as negative control. Among the various molecules tested, only five were able to inhibit 67LR binding to LM (Fig. 11A).

4.11 A molecule identified by a virtual screening is a specific inhibitor of cell binding to laminin

To verify their specificity, the five active compounds were tested by *in vitro* LR-293 cell adhesion to LM, fibronectin (FN) and vitronectin (VN). One compound selectively inhibited LR-293 cell adhesion to LM. This molecule, 1-((4-methoxyphenylamino)methyl)naphthalene-2-ol, identified by the initials NSC47924, decreased cell binding to LM by 85% without affecting cell adherence to FN and VN (Fig.11B).

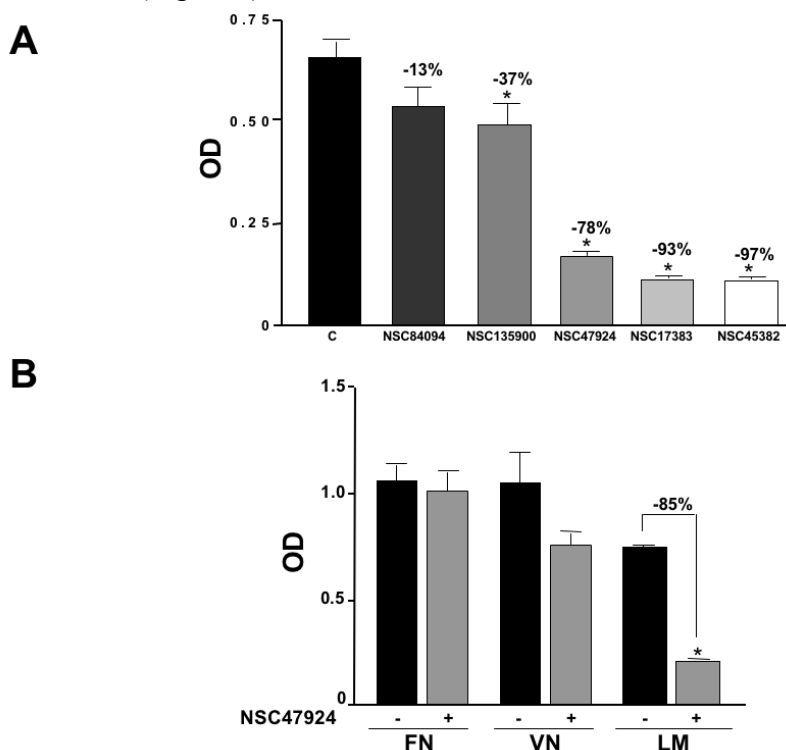


Figure 11. Five top-scoring molecules from the virtual screening of a diversity library of small molecules inhibit LR-293 cell adhesion to laminin; but, only NSC47924 is specific.

A: LR-293 cells were plated in LM-coated wells in the presence of the selected molecules, dissolved in DMSO and added at a concentration of 2×10^{-5} M, corresponding to 10,000-fold 67LR affinity constant for LM; DMSO was used as negative control (■). Attached cells were fixed and stained with crystal violet. The stain was eluted, and the absorbance at 540 nm was measured. The values represent the means+S.D. of three experiments performed in triplicate. (*) $p < 0.05$, as determined by the Student's t test. Only five molecules inhibited LR-293 cell binding to LM.

B: LR-293 cell adhesion to LM, fibronectin (FN) and vitronectin (VN), in the presence of 20 μ M NSC47924 (■) or DMSO, as a negative control (■). The attached cells were fixed and stained with crystal violet. The stain was eluted, and the absorbance at 540 nm was measured. The values represent the means+S.D. of three experiments performed in triplicate. (*) $p < 0.05$, as determined by the Student's t test. 1-((4-methoxyphenylamino)methyl)naphthalene-2-ol, identified by the initials NSC47924, specifically decreased 85% of LR-293 cell binding to LM.

4.12 NSC47924 is a specific inhibitor of 67LR-mediated cell binding to laminin and shows an IC_{50} in the μ molar range

In order to demonstrate the specificity of NSC47924 for 67LR-mediated binding to LM, cell adhesion experiments were performed on V-293 and LR-293 cells. In the presence of NSC47924, the inhibition LM binding was 69% in 67LR-293, compared with 39% observed in control V-293 cells (Fig.12A), that was exactly comparable to the inhibition obtained by anti-67LR antibodies (Fig. 10C). To assess the possibility of using NSC47924 *in vivo*, we calculated its IC_{50} , *i.e.* the concentration of NSC47924 able to inhibit 50% of LR-293 cell binding to LM. LR-293 cell adhesion to LM was evaluated in the presence of increasing concentrations of the inhibitor and the IC_{50} was generated using nonlinear regression of binding curves in GraphPad Prism; it was found at 19.35 μ M (Fig.12B).

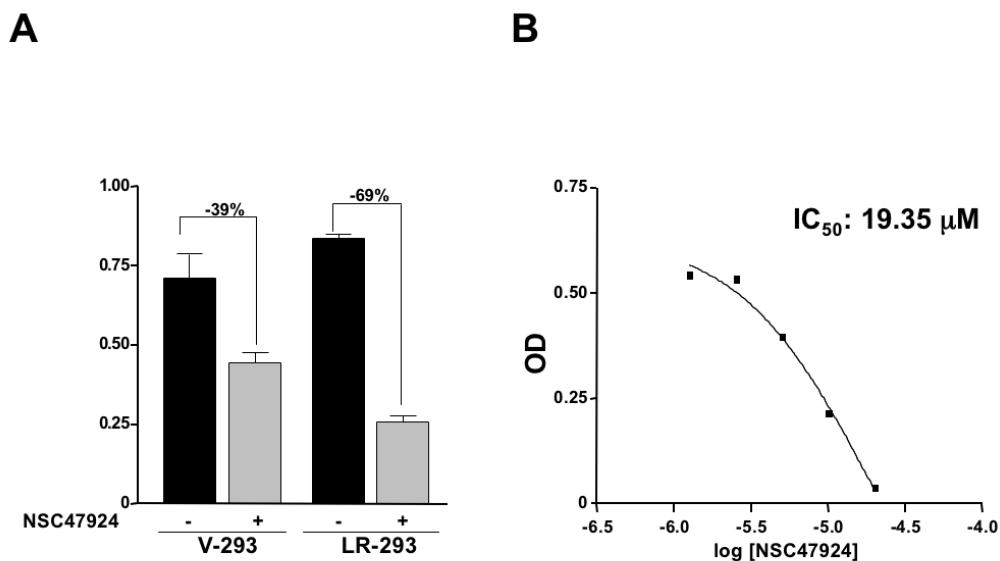


Figure 12. NSC47924 is a specific inhibitor of 67LR-293 cell adhesion to laminin at a low IC_{50} .
A: V-293 and LR-293 cells were plated on LM-coated wells in the presence of 20 μ M NSC47924 (□), or DMSO (■), as a negative control. The attached cells were fixed and stained with crystal violet. The stain was eluted, and the absorbance at 540 nm was measured by a spectrophotometer. The values represent the means+S.D. of three experiments performed in triplicate. (*) $p < 0.05$, as determined by the Student's t test. LM binding inhibition by NSC47924 was comparable to that previously obtained by anti-67LR antibodies.
B: LR-293 cells were plated on LM-coated wells in the presence of increasing concentrations of NSC47924 and the IC_{50} was calculated by GraphPad Prism.

4.13 The specific 67LR inhibitor NSC47924 inhibits cell proliferation, migration and invasion in response to laminin

LM also induces proliferative and migratory signals; therefore, it was investigated whether NSC47924 was able to inhibit cell proliferation and migration/invasion in 67LR overexpressing cells. To this aim, proliferation assays were performed on LR-293 cells after adhesion to LM, in the presence or in the absence of 20 μ M NSC47924. The compound significantly inhibited LR-293 cell the proliferation, as compared to vehicle treated cells (Fig. 13A). In addition, NSC47924 significantly inhibited LR-293 cell migration to LM and matrigel invasion, as compared to vehicle treated cells (Fig. 13B,C).

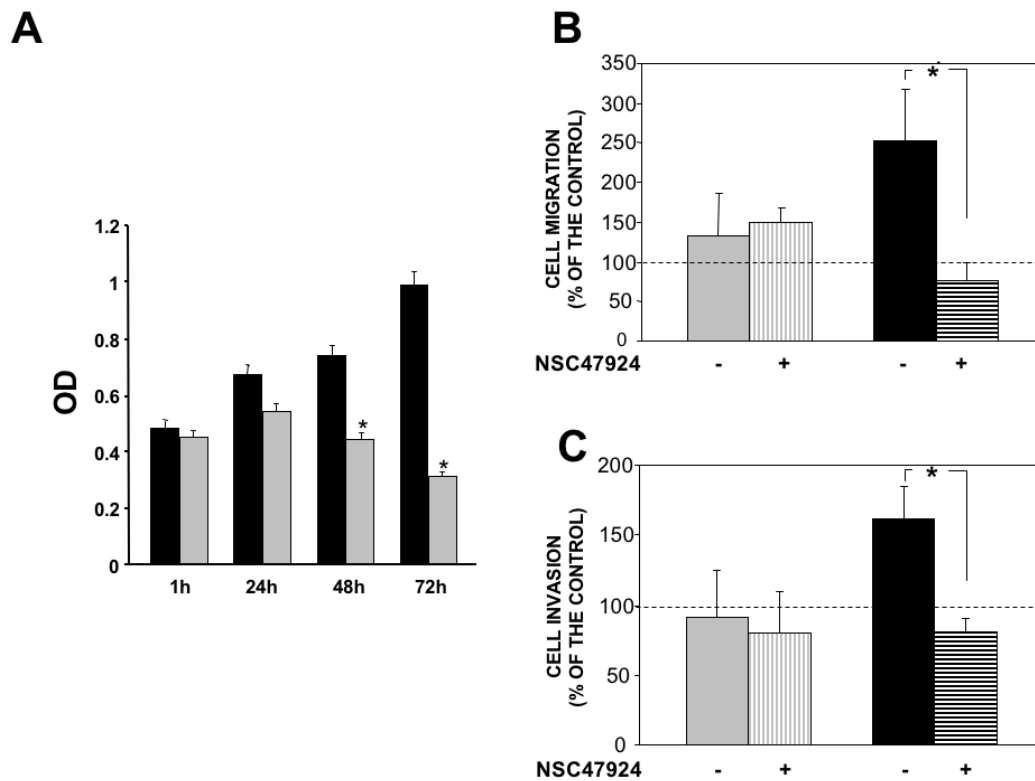


Figure 13. The specific 67LR inhibitor NSC47924 inhibits cell proliferation, migration and invasion in response to laminin.

A: LR-293 were plated on LM-coated wells in the presence of DMSO (■), as a negative control, or 20 μ M NSC47924 (▣). At the indicated times 20 μ l/well of reagent was added and the absorbance (OD) was determined at a wavelength of 490 nm. The values are the mean \pm SD of three experiments performed in triplicate. (*) $p < 0.05$, as determined by the Student's *t* test.

B: V-293 cells (▣) LR-293 cells (■) were pre-incubated with DMSO (-) or 20 μ M NSC47924 (+), plated in Boyden chambers and allowed to migrate toward 50 μ g/ml LM on filters coated with 10 μ g/ml FN. The values are the mean \pm SD of three experiments performed in triplicate. (*) $p < 0.05$, as determined by the Student's *t* test.

C: V-293 cells (▣) and LR-293 cells (■) were preincubated with DMSO (-) or 20 μ M NSC47924 (+), plated in Boyden chambers and allowed to invade matrigelTM. The values are the mean \pm SD of three experiments performed in triplicate. (*) $p < 0.05$, as determined by the Student's *t* test. NSC47924 significantly inhibited LR-293 cell proliferation, migration and invasion in response to LM.

5.CONCLUSION

By yeast two hybrid screening, the 67 kDa laminin receptor (67LR) was identified as a new candidate partner of the anti-apoptotic protein phosphoprotein enriched in diabetes/phosphoprotein enriched in astrocytes (PED/PEA-15). In this study, we confirmed the interaction between 67LR and PED/PEA-15, through pull down and immunoprecipitation experiments, using both exogenous and endogenous proteins. Then, we investigated the effects of PED/PEA-15 overexpression, occurring in different human tumors, such as breast and lung cancer, on 67LR-mediated cell functions, namely, cell adhesion and migration to LM and matrigel invasion. We also investigated the downstream effects of PED/PEA-15 and 67LR interaction on extracellular matrix-derived signal transduction pathways.

We showed for the first time that PED overexpression increases cell adhesion and migration to LM, the major component of basal membranes, through its interaction with 67LR. This effect is mediated by increased 67LR binding to LM, ERK1/2 phosphorylation and Rac1 activation. Therefore, a PED/PEA-15 dependent signal transduction pathway, usually activated in response to growth factor stimulation (Zanca 2010), is also activated after cell adhesion to basement membranes, a prerequisite for tumor invasion and metastasis.

PED/PEA-15 is involved in promoting cell migration and invasion, through its interaction with 67LR. Interestingly, it has been recently reported that 67LR is overexpressed in astrocytoma and its downregulation reduces the migratory activity of human glioma cells (Chen 2009). Findings on PED/PEA-15 are more controversial; it has been described a PED/PEA-15 mediated inhibition of cell migration/invasion in astrocytoma (Renault-Mihara 2006) whereas an increase has been shown in NSCLC (Zanca 2010). Our data confirm the last report.

67LR is also involved in the regulation of cell proliferation and survival. Indeed, reduction of 67LR expression in HeLa cells results in apoptosis (Kaneda 1998); apoptosis is also observed in Hep3B cells upon reduction of 67LR (Susantad 2008). 67LR has been implicated in cell signalling pathways that are important for cell survival as well (Givant-Horwitz 2004), making it a suitable target for novel cancer gene therapy (Scheiman 2010).

In that regard, we demonstrated that 67LR and PED/PEA-15 interfere with each other's function once bound together. In fact, PED/PEA-15 interaction with 67LR increases cell adhesion, migration and invasion to LM. When 67LR is active, it promotes PKC and CAMKII activation. Active PKC facilitates PED/PEA-15 phosphorylation on Ser104 and the consequent release of ERKs to the nucleus, thus allowing cell proliferation that, in PED/PEA-15 overexpressing cells is slowed (Glading 2007; Zanca 2010). Active CAMKII facilitates PED/PEA-15 phosphorylation on Ser116, thus enhancing the binding to DED containing

proteins and caspase 8 (Renganathan 2005; Kubes 1998; Trencia 2003) and inhibiting of apoptosis.

Therefore, a PED/PEA-15 dependent signal transduction pathway, leading to cell proliferation and resistance to apoptosis and usually activated in response to growth factor stimulation, is also activated after 67LR mediated cell adhesion to basement membranes, a prerequisite for tumor invasion and metastasis.

These considerations prompted us to search for small molecules that might target 67LR activities. We conducted a computational screening of a diversity library of small molecules using the recently solved 67LR crystal structure, focusing on residues showed to be important for laminin binding. This analysis identified a lead compound, NSC47924, that specifically inhibited cell adhesion, migration, invasion and proliferation in response to LM in 67LR overexpressing cells.

Since cancer cells overexpress 67LR, we expect this compound to be cancer cell specific and minimally toxic. Therefore, we are now evaluating NSC47924 in vivo activity by in vivo tumorigenicity and metastasis assay.

This lead compound could be the basis for the development of a new class of anti-cancer drugs, specifically targeting cell invasion and metastasis.

6. REFERENCES

- Ardini E, Tagliabue E, Magnifico A, Butò S, Castronovo V, Colnaghi MI, Ménard S. Co-regulation and physical association of the 67 kD monomeric laminin receptor and the $\alpha 6\beta 4$ integrin. *J Biol Chem* 1997; 272: 2342-2345.
- Ardini E, Pesole G, Tagliabue E, Magnifico A, Castronovo V, Sobel ME, Colnaghi MI, Ménard S. The 67-kDa laminin receptor originated from a ribosomal protein that acquired a dual function during evolution. *Mol Biol Evol* 1998; 15 : 1017-1025.
- Ardini E, Sporchia B, Pollegioni L, Modugno M, Ghirelli C, Castiglioni F, Tagliabue E, Menard S. Identification of a novel function for 67-kDa laminin receptor: increase in laminin degradation rate and release of motility fragments. *Cancer Res* 2002; 62:1321-1325.
- Auth D, Brawerman G. A 33-kDa polypeptide with homology to the laminin receptor: component of translation machinery. *Proc Natl Acad Sci U S A.* 1992; 89: 4368-4372.
- Berno V, Porrini D, Castiglioni F, Campiglio M, Casalini P, Pupa SM, Balsari A, Menard S, Tagliabue E. The 67 kDa laminin receptor increases tumor aggressiveness by remodeling laminin-1. *Endocr Relat Cancer* 2005; 12: 393-406.
- Butò S, Tagliabue E, Ardini E, Magnifico A, Ghirelli C, van den Brùle F, Castronovo V, Colnaghi MI, Sobel ME, Ménard S. Formation of the 67-kDa laminin receptor by acylation of the precursor. *J Cell Biochem.* 1998; 69: 244-251.
- Callaway K, Abramczyk O, Martin L, Dalby KN. The anti-apoptotic protein PEA-15 is a tight binding inhibitor of ERK1 and ERK2, which blocks docking interactions at the D-recruitment site. *Biochemistry* 2007; 46: 9187–9198.
- Castronovo V, Taraboletti G, Sobel ME. Functional domains of the 67kDa laminin receptor precursor. *J Biol Chem* 1991; 266: 20440-20446.
- Chen A, Ganor Y, Rahimipour S, Ben-Aroya N, Koch Y, Levite M. The neuropeptides GnRH-II and GnRH-I are produced by human T cell and trigger laminin receptor gene expression, adhesion, chemotaxis and homing to specific organs. *Nat Med* 2002; 8: 1421-1426.
- Chen FX, Qian YR, Duan YH, Ren WW, Yang Y, Zhang CC, Qiu YM, Ji YH.

Down-regulation of 67LR reduces the migratory activity of human glioma cells in vitro. *Brain Res Bull* 2009; 79: 402-408.

Chou FL, Hill JM, Hsieh JC, Pouyssegur J, Brunet A, Glading A, Uberall F, Ramos JW, Werner MH, Ginsberg MH. PEA-15 binding to ERK1/2 MAPKs is required for its modulation of integrin activation. *J Biol Chem* 2003; 278: 52587-52597.

Condorelli G, Vigliotta G, Iavarone C, Caruso M, Tocchetti CG, Andreozzi F, Cafieri A, Tecce MF, Formisano P, Beguinot L, Beguinot F. PED/PEA-15 gene controls glucose transport and is overexpressed in type 2 diabetes mellitus. *EMBO J* 1998; 17: 3858-3866.

Condorelli G, Vigliotta G, Cafieri A, Trencia A, Andalo` P, Oriente F, Miele C, Caruso M, Formisano P, Beguinot F. PED/PEA-15: an anti-apoptotic molecule that regulates FAS/TNFR1-induced apoptosis. *Oncogene* 1999; 18: 4409-4415.

Duan SG, Cheng L, Li DJ, Zhu J, Xiong Y, Li XW, Wang SG. The role of MAPK-ERK pathway in 67-kDa laminin receptor-induced FasL expression in human cholangiocarcinoma cells. *Dig Dis Sci* 2010; 55:2844-2852.

Eblen ST, Slack JK, Weber MJ, Catling AD. Rac-PAK signaling stimulates extracellular signal-regulated kinase (ERK) activation by regulating formation of MEK1-ERK complexes. *Mol Cell Biol* 2002; 22: 6023-6033.

Eckert A, Böck BC, Tagscherer KE, Haas TL, Grund K, Sykora J, Herold-Mende C, Ehemann V, Hollstein M, Chneiweiss H, Wiestler OD, Walczak H, Roth W. The PEA-15/PED protein protects glioblastoma cells from glucose deprivation-induced apoptosis via the ERK/MAP kinase pathway. *Oncogene* 2008; 27: 1155-1166.

Fiory F, Formisano P, Perruolo G, Beguinot F. *Frontiers: PED/PEA-15, a multifunctional protein controlling cell survival and glucose metabolism. Am J Physiol Endocrinol Metab* 2009; 297: E592-601.

Ford CL, Randal-Whitis L, Ellis SR. Yeast proteins related to the p40/laminin receptor precursor are required for 20S ribosomal RNA processing and the maturation of 40S ribosomal subunits. *Cancer Res* 1999; 59: 704-710.

Formisano P, Perruolo G, Libertini S, Santopietro S, Troncone G, Raciti GA, Oriente F, Portella G, Miele C, Beguinot F. Raised expression of the antiapoptotic

protein ped/pea-15 increases susceptibility to chemically induced skin tumor development. *Oncogene* 2005; 24: 7012–7021.

Formstecher E, Ramos JW, Fauquet M, Calderwood DA, Hsieh JC, Canton B, Nguyen XT, Barnier JV, Camonis J, Ginsberg MH, Chneiweiss H. PEA-15 mediates cytoplasmic sequestration of ERK MAP kinase. *Dev Cell* 2001; 1: 239–250.

Garofalo M, Romano G, Quintavalle C, Romano MF, Chiurazzi F, Zanca C, Condorelli G. Selective inhibition of PED protein expression sensitizes B-cell chronic lymphocytic leukaemia cells to TRAIL-induced apoptosis. *Int J Cancer* 2007; 120: 1215-1222.

Gauczynski S, Peyrin JM, Haïk S, Leucht C, Hundt C, Rieger R, Krasemann S, Deslys JP, Dormont D, Lasmézas CI, Weiss S. The 37-kDa/67-kDa laminin receptor acts as the cell-surface receptor for the cellular prion protein. *EMBO J*. 2001; 20: 5863-5875.

Giannelli G, Falk-Marzillier J, Schiraldi O, Stetler-Stevenson WG, Quaranta V. Induction of cell migration by matrix metalloprotease-2 cleavage of laminin-5. *Science*. 1997; 277: 225-228.

Gietz D, St Jean A, Woods RA, Schiestl RH. Improved method for high efficiency transformation of intact yeast cells. *Nucleic Acids Res* 1992; 20:1425.

Givant-Horwitz V, Davidson B, Reich R. Laminin-induced signaling in tumor cells: the role of the M(r) 67,000 laminin receptor. *Cancer Res* 2004; 64: 3572–3579.

Glading A, Koziol JA, Krueger J, Ginsberg MH. PEA-15 inhibits tumor cell invasion by binding to extracellular signal-regulated kinase 1/2. *J Biol Chem* 2007; 279: 46802–46809.

Graf J, Ogle RC, Robey FA, Sasaki M, Martin GR, Yamada Y, Kleinman HK. A pentapeptide from the laminin B1 chain mediates cell adhesion and binds the 67,000 laminin receptor. *Biochemistry* 1987; 26: 6896–6900.

Hao C, Beguinot F, Condorelli G, Trencia A, Van Meir EG, Yong VW, Parney IF, Roa WH, Petruk KC. Induction and intracellular regulation of tumor necrosis factor-related apoptosis-inducing ligand (TRAIL) mediated apoptosis in human malignant glioma cells. *Cancer Res* 2001; 61: 1162–1170.

Holtl L, Zelle-Rieser C, Gander H, Papesh C, Ramoner R, Bartsch G, Rogatsch H, Barsoum AL, Coggin JH, Thurnher M. Immunotherapy of metastatic renal cell carcinoma with tumor lysate-pulsed autologous dendritic cells. *Clin Cancer Res.* 2002; 8: 3369-3376.

Jackers P, Minoletti F, Belotti D, Clausse N, Sozzi G, Sobel ME, Castronovo V. Isolation from a multigene family of the active human gene of the metastasis-associated multifunctional protein 37LRP/p40 at chromosome 3p21.3. *Oncogene* 1996; 13: 495-503.

Jamieson KV, Wu J, Hubbard SR, Meruelo D. Crystal structure of the human laminin receptor precursor *J Biol Chem* 2008; 283: 3002-3005.

Jamieson KV, Hubbard SR, Meruelo D. Structure-Guided Identification of a Laminin Binding Site on the Laminin Receptor Precursor. *J Mol Biol.* 2010.

Kaneda Y, Kinoshita K, Sato M, Saeki Y, Yamada R, Wataya-Kaneda M et al. The induction of apoptosis in HeLa cells by the loss of LBP-p40. *Cell Death Differ* 1998; 5: 20–28.

Kazmin DA, Hoyt TR, Taubner L, Teintze M, Starkey JR. Phage display mapping for peptide 11 sensitive sequences binding to laminin-1. *J Mol Biol* 2000; 298: 431-445.

Kinoshita K, Kaneda Y, Sato M, Saeki Y, Wataya-Kaneda M, Hoffmann A. LBP-p40 binds DNA tightly through associations with histones H2A, H2B, and H4. *Biochem Biophys Res Commun* 1998; 253: 277-282.

Kitsberg D, Formstecher E, Fauquet M, Kubes M, Cordier J, Canton B, Pan G, Rolli M, Glowinski J, Chneiweiss H. Knock-out of the neural death effector domain protein PEA-15 demonstrates that its expression protects astrocytes from TNFalpha-induced apoptosis. *J Neurosci* 1999; 19: 8244–8251.

Koliakos KK, Sapountzi Z, Papageorgiou A, Trachana V, Kotsinou S, Koliakos G. Antiidiotypic antibodies carrying the “internal image” of peptide YIGSR inhibit spontaneous metastasis of Lewis lung carcinoma in mice. *In vivo* 2002; 16: 511-518.

Krueger J, Chou FL, Glading A, Schaefer E, Ginsberg MH. Phosphorylation of phosphoprotein enriched in astrocytes (PEA-15) regulates extracellular signal-regulated kinase-dependent transcription and cell proliferation. *Mol Biol Cell*

2005; 16: 3552-3561.

Kubes M, Cordier J, Glowinski J, Girault JA, Chneiweiss H. Endothelin induces a calcium-dependent phosphorylation of PEA-15 in intact astrocytes: identification of Ser104 and Ser116 phosphorylated, respectively, by protein kinase C and calcium/calmodulin kinase II in vitro. *J Neurochem* 1998; 71: 1307–1314.

Landowski TH, Dratz EA, Starkey JR. Studies of the structure of the metastasis-associated 67 kDa laminin binding protein: fatty acid acylation and evidence supporting dimerization of the 32 kDa gene product to form the mature protein. *Biochemistry* 1995; 34: 11276-11287.

Magnifico A, Tagliabue E, Butò S, Ardini E, Castronovo V, Colnaghi MI, Ménard S. Peptide G, containing the binding site of the 67 kDa laminin receptor, increases and stabilizes laminin binding to cancer cells. *J Biol Chem* 1996; 271: 31179-31184.

Massia SP, Rao SS, Hubbell JA. Covalently immobilized laminin peptide Tyr-Ile-Gly-Ser-Arg (YIGSR) supports cell spreading and co-localization of the 67-kilodalton laminin receptor with alpha-actinin and vinculin. *J Biol Chem.* 1993; 268: 8053-8059.

Mecham RP, Receptors for laminin on mammalian cells. *FASEB J* 1991; 5: 2538–2546.

Menard S, Tagliabue E, Colnaghi MI. The 67 kDa laminin receptor as a prognostic factor in human cancer. *Breast Cancer Res Treat* 1998; 52: 137–145.

Miller JH. *Experiments in Molecular Genetics* (1972). Cold Spring Harbor Laboratory, Cold Spring Harbor, NY

Montuori N, Sobel ME. The 67-kDa laminin receptor and tumor progression. *Curr Top Microbiol Immunol* 1996; 213: 205-214.

Montuori N, Selleri C, Risitano AM, Raiola AM, Ragno P, Del Vecchio L, Rotoli B, Rossi G. Expression of the 67-kDa Laminin Receptor in acute myeloid leukemia cells mediates adhesion to laminin and is frequently associated with monocytic differentiation. *Clin Cancer Res* 1999; 5: 1465-1472.

- Nelson J, McFerran NV, Pivato G, Chambers E, Doherty C, Steele D, Timson DJ. The 67 kDa laminin receptor: structure, function and role in disease. *Biosci Rep* 2008; 28: 33-48.
- Pierri CL, Parisi G, Porcelli V. Computational approaches for protein function prediction: A combined strategy from multiple sequence alignment to molecular docking-based virtual screening. *Biochim Biophys Acta* 2010; 1804: 1695-1712.
- Ramos JW, Hughes PE, Renshaw MW, Schwartz MA, Formstecher E, Chneiweiss H, Ginsberg MH. Death effector domain protein PEA-15 potentiates Ras activation of extracellular signal receptor-activated kinase by an adhesion-independent mechanism. *Mol Biol Cell* 2000; 11: 2863–2872.
- Rao CN, Castronovo V, Schmitt MC, Wewer UM, Claysmith AP, Liotta LA, Sobel ME. Evidence for a precursor of the high-affinity metastasis-associated murine laminin receptor. *Biochemistry* 1989; 28:7476-7486.
- Rao NC, Barsky SH, Terranova VP and Liotta LA. Isolation of a tumor cell laminin receptor. *Biochem Biophys Res Commun.*1983; 111: 804–808.
- Reddy KB, Nabha SM, Atanaskova N. Role of MAP kinase in tumor progression and invasion. *Cancer Metastasis Rev* 2003; 22: 395–403.
- Renault-Mihara F, Beuvon F, Iturrioz X, Canton B, De Bouard S, Léonard N, Mouhamad S, Sharif A, Ramos JW, Junier MP, Chneiweiss H. Phosphoprotein enriched in astrocytes-15 kDa expression inhibits astrocyte migration by a protein kinase C delta-dependent mechanism. *Mol Biol Cell* 2006; 17: 5141-5152.
- Renganathan H, Vaidyanathan H, Knapinska A, Ramos JW. Phosphorylation of PEA-15 switches its binding specificity from ERK/MAPK to FADD. *Biochem J* 2005; 390: 729–735.
- Satoh K, Narumi K, Abe T, Sakai T, Kikuchi T, Tanaka M, Shimo-Oka T, Uchida M, Tezuka F, Isemura M, Nukiwa T. Diminution of 37-kDa laminin binding protein expression reduces tumor formation of murine lung cancer cells. *Br J Cancer.* 1999; 80: 1115-1122.
- Scheiman J, Tseng JC, Zheng Y, Meruelo D. Multiple functions of the 37/67-kd laminin receptor make it a suitable target for novel cancer gene therapy. *Mol Ther* 2010; 18: 63-74.

Susantad T, Smith DR. siRNA-mediated silencing of the 37/67-kDa high affinity laminin receptor in Hep3B cells induces apoptosis. *Cell Mol Biol Lett* 2008; 13: 452–464.

Taraboletti G, Belotti D, Giavazzi R, Sobel ME, Castronovo V. Enhancement of metastatic potential of murine and human melanoma cells by laminin receptor peptide G: attachment of cancer cells to subendothelial matrix as a pathway for hematogenous metastasis. *J Natl Cancer Inst* 1993; 85: 235–240.

Têtu B, Brisson J, Lapointe H, Wang CS, Bernard P, Blanchette C. Cathepsin D expression by cancer and stromal cells in breast cancer: an immunohistochemical study of 1348 cases. *Breast Cancer Res Treat.* 1999; 55:137-147.

Todaro M, Zerilli M, Ricci-Vitiani L, Bini M, Perez Alea M, Maria Florena A, Miceli L, Condorelli G, Bonventre S, Di Gesù G, De Maria R, Stassi G. Autocrine production of interleukin-4 and interleukin-10 is required for survival and growth of thyroid cancer cells. *Cancer Res* 2006; 66:1491-1499.

Trencia A, Perfetti A, Cassese A, Vigliotta G, Miele C, Oriente F, Santopietro S, Giacco F, Condorelli G, Formisano P, Beguinot F. Protein kinase B/Akt binds and phosphorylates PED/PEA-15, stabilizing its antiapoptotic action. *Mol Cell Biol* 2003; 23: 4511–4521.

Wewer UM, Taraboletti G, Sobel ME, Albrechtsen R, Liotta LA. Role of laminin receptor in tumor cell migration. *Cancer Res* 1987; 47: 5691-5698.

Yan S, Sameni M, Sloane BF. Cathepsin B and human tumor progression. *Biol Chem.* 1998; 379: 113-123.

Zanca C, Garofalo M, Quintavalle C, Romano G, Acunzo M, Ragno P, Montuori N, Incoronato M, Tornillo L, Baumhoer D, Briguori C, Terracciano L, Condorelli G. PED is overexpressed and mediates TRAIL resistance in human non-small cell lung cancer. *J Cell Mol Med* 2008; 12: 2416-2426.

Zanca C, Cozzolino F, Quintavalle C, Di Costanzo S, Ricci-Vitiani L, Santoriello M, Monti M, Pucci P, Condorelli G. PED interacts with Rac1 and regulates cell migration/invasion processes in human non-small cell lung cancer cells. *J Cell Physiol* 2010; 225: 63-72.

Zuber C, Knackmuss S, Zemora G, Reusch U, Vlasova E, Diehl D, Mick V, Hoffmann K, Nikles D, Fröhlich T, Arnold GJ, Brenig B, Wolf E, Lahm H, Little

M, Weiss S. Invasion of tumorigenic HT1080 cells is impeded by blocking or downregulating the 37-kDa/67-kDa laminin receptor. *J Mol Biol* 2008; 378: 530-539.

Zuber C, Knackmuss S , Rey C, Reusch U, Röttgen P, Fröhlich T, Arnold GJ, Pace C, Mitteregger G, Kretzschmar HA, Little M, Weiss S Single chain Fv antibodies directed against the 37 kDa/67 kDa laminin receptor as therapeutic tools in prion diseases. *Molecular Immunology* 2008; 45: 144–151.

The cross-talk between the urokinase receptor and fMLP receptors regulates the activity of the CXCR4 chemokine receptor

Nunzia Montuori · Katia Bifulco · Maria Vincenza Carriero ·
Claudio La Penna · Valeria Visconte · Daniela Alfano · Ada Pesapane ·
Francesca Wanda Rossi · Salvatore Salzano · Guido Rossi · Pia Ragno

Received: 27 May 2010 / Revised: 10 September 2010 / Accepted: 7 October 2010
© Springer Basel AG 2010

Abstract The receptor (CXCR4) for the stromal-derived factor-1 (SDF1) and the urokinase-receptor (uPAR) are up-regulated in various tumors. We show that CXCR4-transfected cells migrate toward SDF1 on collagen (CG) and do not on vitronectin (VN). Co-expression of cell-surface uPAR, which is a VN receptor, impairs SDF1-induced migration on CG and allows migration on VN. Blocking fMLP receptors (fMLP-R), alpha-v integrins or the uPAR region capable to interact with fMLP-Rs, impairs migration of uPAR/CXCR4-transfected cells on VN and restores their migration on CG. uPAR co-expression also reduces the adherence of CXCR4-expressing cells to various components of the extracellular matrix (ECM) and influences the partitioning of beta1 and alpha-v integrins to membrane lipid-rafts, affecting ECM-dependent signaling. uPAR

interference in CXCR4 activity has been confirmed in cells from prostate carcinoma. Our results demonstrate that uPAR expression regulates the adhesive and migratory ability of CXCR4-expressing cells through a mechanism involving fMLP receptors and alpha-v integrins.

Keywords uPAR · Urokinase-receptor · fMLP receptors · CXCR4 · Prostate carcinoma cells

Introduction

The CXCR4 chemokine receptor is implicated in several physiologic and pathologic processes; in fact, it is a co-receptor for T-trophic HIV, plays a fundamental role in fetal development and in the trafficking of naive lymphocytes, and is a key molecule in the regulation of hematopoietic stem cell (HSC) trafficking from and to the bone marrow (BM). In fact, CXCR4 is expressed in HSCs, and its ligand, the stromal derived factor 1 (SDF1), is largely produced by BM endothelium [1].

CXCR4 and SDF1 are also considered key molecules in invasion and metastasis of several cancers. CXCR4 is highly expressed by several tumors such as leukemias, breast, prostate, lung and brain tumors, and is strongly involved in directing tumor cells to organs that highly express SDF1 (lymph nodes, lungs, liver, bones), which contributes to a suitable microenvironment for metastatic cells [2–5].

Urokinase (uPA) is a serine protease that activates plasminogen to plasmin and binds a specific high-affinity cell-surface receptor, uPAR [6]. uPAR is formed by three homologous domains (D1, D2, D3) anchored to the cell surface by a glycosyl-phosphatidylinositol (GPI) tail. The GPI-anchor confers extreme mobility to uPAR along the

N. Montuori and K. Bifulco contributed equally to this work.

N. Montuori · C. La Penna · V. Visconte · A. Pesapane ·
G. Rossi
Department of Cellular and Molecular Biology and Pathology,
"Federico II" University, Naples, Italy

K. Bifulco · M. V. Carriero
Department of Experimental Oncology,
National Cancer Institute, Naples, Italy

D. Alfano · P. Ragno (✉)
Department of Chemistry, University of Salerno,
Via Ponte don Melillo, 84084 Fisciano (Salerno), Italy
e-mail: pragno@unisa.it

F. W. Rossi
Department of Clinical Immunology and Allergy,
"Federico II" University, Naples, Italy

S. Salzano
Institute of Experimental Endocrinology and Oncology
(National Research Council), Naples, Italy

Published online: 24 October 2010

cell membrane and allows its association to lipid rafts, cholesterol-rich microdomains of the plasma membrane, which seem implicated in signal transduction events initiated by cell adhesion to the extracellular matrix (ECM) [7, 8].

uPAR is strongly up-regulated in several cancers and represents a negative prognostic factor [9]. uPAR traditional role was considered the focusing of proteolytic uPA activity on the cell membrane. However, proteolysis-independent uPAR activities have been demonstrated in the last years [9]. uPAR binds vitronectin, a component abundant in tumor-associated ECM [10, 11], interacts with various integrins regulating their activity, interferes with the activity of specific growth-factor receptors, mediates uPA-dependent cell migration and is required for chemotaxis induced by fMet-Leu-Phe (fMLP), a potent leukocyte chemoattractant [9, 12]. Indeed, cell-surface uPAR functionally interacts with fMLP-receptors (fMLP-Rs) through a specific site corresponding to amino acids 88–92 (SRSRY) located in the region linking uPAR domain 1 (D1) to uPAR domain 2 (D2) [13, 14]. The fMLP receptor family comprises three highly homologous receptors: the high and low affinity fMLP-Rs, FPR and FPRL1, and the FPRL2, which does not bind fMLP [15].

uPAR can be cleaved, thus generating cell-surface truncated forms lacking the N-terminal D1 domain. uPAR cleavage negatively regulates most of full-length uPAR activities, since cleaved uPAR does not bind uPA and VN, and does not coimmunoprecipitate with integrins. Nevertheless, cleaved uPAR, still containing the SRSRY sequence at its N-terminus, retains its ability to functionally interact with fMLP-Rs [9, 12].

Both full-length and cleaved uPAR forms can be shed from the cell surface, generating soluble full-length (suPAR) and cleaved (c-suPAR) forms of uPAR. The soluble form of cleaved uPAR, lacking the N-terminal domain and exposing residues 88–92 (SRSRY-c-suPAR), or soluble uPAR peptides, containing the SRSRY sequence, are ligands for all three fMLP-Rs and induce migration of various cell types, including HSCs [13, 16, 17]. The SRSRY-dependent signaling is supported by a cross-talk between the high-affinity fMLP receptor (FPR) and the α -v chain of integrin VN receptors [18]. SRSRY-c-suPAR also regulates the activity of inflammatory chemokine receptors, such as MCP-1 and RANTES receptors, through fMLP-R activation [19].

Independently on uPAR expression, fMLP-Rs have been reported to regulate the activity of other chemokine receptors, including CXCR4 [20–22] and integrins [23]. Recently, increased expression of fMLP-Rs in some tumors has been demonstrated [24].

We recently demonstrated that the suPAR derived peptide, uPAR₈₄₋₉₅, (residues 84–95), containing the

SRSRY sequence, is able to mobilize murine HSCs from BM into the circulation, likely by stimulating HSC migration and/or by impairing migration of human and mouse leukemia cells toward the CXCR4 ligand, SDF1 [17, 25].

These observations prompted us to investigate whether the cell-surface uPAR can interfere with CXCR4 activity, by examining the effect of uPAR expression on CXCR4 functions.

Materials and methods

Reagents

The rabbit anti-uPAR polyclonal antibody and the amino-terminal fragment of uPA (ATF) were from American Diagnostica (Greenwich, CT); the monoclonal antibody R4 was kindly provided by Dr. G. Hoyer-Hansen (Finsen Laboratory, Copenhagen, Denmark). Rabbit polyclonal antibodies against α -v and β tal integrins, the polyclonal antibody directed to phosphorylated ERK 1/2 and the monoclonal antibody against total ERK 2 used in Western-blot analysis, were from Santa Cruz Biotechnology (Santa Cruz, CA); the anti- α -v integrin monoclonal antibody (P3G8) used in migration assays was from Chemicon (Temecula, CA); the rabbit polyclonal antibody directed to the N-terminus of CXCR4 was from Upstate (Temecula, CA). FITC-anti-mouse IgG were purchased from Santa Cruz Biotechnology and Alexa Fluor 594 anti-rabbit IgG from Invitrogen (Carlsbad, CA, USA). Horseradish peroxidase-conjugated anti-mouse and anti-rabbit IgG were from Bio-Rad (Hercules, CA); fluorescein isothiocyanate-labeled goat anti-rabbit IgG were from Jackson Lab (West Grove, PA). ECL detection kit was from Amersham Biosciences. Polyvinylidene fluoride (PVDF) filters were from Millipore (Windsor, MA). Collagen, laminin, fibronectin were from Collaborative Biotech (Bedford, MA) and vitronectin from Promega (Madison, WI). The chemotaxis polyvinylpyrrolidone-free (PVPF) filters were from Whatman Int. (Kent, UK) and 96-well flat-bottom microtiter plates were from NUNC (Roskilde, Denmark). uPAR-specific siRNA and the control siRNA were from Qiagen (Valencia, CA, USA); oligofectamine and lipofectamine from Invitrogen. The WKYMVm peptide was synthesized by Innovagen (Lund, Sweden). The rabbit antibody recognizing the SRSRY sequence of uPAR has been developed by PRIMM (Milan, Italy) by using the uPAR₈₄₋₉₅ peptide (corresponding to uPAR residues 84–95, which include the SRSRY sequence) assembled onto a branching lysine core. The antibody specificity and sensitivity was tested by ELISA; 10 μ g/ml of antibody detected up to 2 ng of uPAR₈₄₋₉₅ peptide.

Cell culture

Human embryonic kidney 293 (HEK-293) cells were grown in DMEM and PC3 prostate carcinoma cells in RPMI, supplemented with 10% fetal bovine serum (FBS). Transfected cells were grown in DMEM supplemented with 10% FBS and selective antibiotics.

Transfection

uPAR cDNA was cloned in a pcDNA3 vector with resistance to Geneticin, and the resulting plasmid was named uPAR-pcDNA3 [14]. The cDNA coding for CXCR4, cloned in a pcDNA3 vector with resistance to Hygromycin, named CXCR4-pcDNA3, was kindly provided by Dr. R.M. Melillo ("Federico II" University, Naples, Italy). A total of 5×10^6 cells, cultured overnight in 100 mm tissue culture dishes, were transfected with 10 μ g of uPAR-pcDNA3 or with the empty vector pcDNA3 by 60 μ l of Lipofectamine for 5 h at 37°C (5% CO₂). Transfected cells were selected by Geneticin at 1.5 mg/ml for 15 days, pooled and cultured in the presence of 0.5 mg/ml Geneticin. uPAR- and vector-transfected cells were then transfected again with CXCR4-pcDNA3 or the empty vector pcDNA3 resistant to Hygromycin. Double transfected cells (uPAR/CXCR4-293, CXCR4-293, V-293) were selected by Hygromycin at 0.4 mg/ml for 15 days and then cultured in the presence of 0.5 mg/ml Geneticin and 0.2 mg/ml Hygromycin.

Flow cytometry analysis

The cells were harvested by 2 mM EDTA-PBS and washed in Ca²⁺/Mg²⁺-containing PBS. 5×10^5 cells were incubated with 10 μ g/ml of anti-uPAR or anti-CXCR4 polyclonal antibodies for 1 h at 4°C. Purified rabbit immunoglobulins were used as a negative control. The cells were then washed and incubated with a fluorescein isothiocyanate-labeled goat anti-rabbit IgG for 30 min at 4°C. Finally, the cells were washed and analyzed by flow cytometry using a FACScan (Becton-Dickinson, Mountain View, CA).

Fluorescence microscopy

Transfected cells were grown on glass slides and stimulated with 100 ng/ml SDF1 or DMEM for 1 h at 37°C. Then, the cells were incubated for 2 h at 20°C with the R4 mouse uPAR-specific antibody (2 μ g/ml) and a rabbit CXCR4-specific antibody (10 μ g/ml) or nonimmune Ig, washed and further incubated for 1 h at 20°C with FITC anti-mouse IgG (1:100) and Alexa Fluor 594 anti-rabbit IgG (1:200). Cells were visualized using a Zeiss 510META LSM microscope in multitrack analysis.

In internalization experiments with fluorescent *N*-formyl-Nle-Leu-Phe-Nle-Tyr-Lys, the cells, grown on glass slides to semi-confluence, were incubated with buffer, 100 nM fMLP, 100 nM uPAR₈₄₋₉₅ peptide or 100 nM scrambled peptide for 30 min at 37°C. Then, the cells were washed with PBS, exposed to 10 nM fluorescent *N*-formyl-Nle-Leu-Phe-Nle-Tyr-Lys (Molecular Probes) for an additional 30 min at 37°C. Cells were visualized using a Zeiss 510META LSM microscope. Z-series images represent focal planes corresponding to 0.5 μ m vertical interval.

Cell migration assay

Cell migration assays were performed in Boyden chambers using 8- μ m-pore-size PVPF polycarbonate filters coated with 5 μ g/ml of vitronectin, collagen, fibronectin, or laminin. Transfected cells (2×10^5) were plated in the upper chamber in serum-free medium. 100 nM SDF1 or serum free medium was added in the lower chamber. The cells were allowed to migrate for 4 h at 37°C, 5% CO₂. The cells on the lower surface of the filter were then fixed in ethanol, stained with hematoxylin, and counted at 200 \times magnification (ten random fields/filter). In a separate set of experiments, transfected cells were preincubated for 1 h at room temperature with 5 μ g/ml of polyclonal antibodies directed to uPAR or the uPAR₈₄₋₉₅ region or 5 μ g/ml of a monoclonal antibody directed to α -v integrins, or for 1 h at 37°C with 100 nM fMLP, 100 nM uPAR₈₄₋₉₅ peptide or 5 nM WKYMVm peptide.

In migration assays with PC3 cells, 1×10^5 cells/filter were loaded and the cells were allowed to migrate for 2 h at 37°C, 5% CO₂. In migration assays with uPAR-silenced PC3 cells, cells have been transfected with 50 nM uPAR-specific siRNA or control siRNA oligonucleotides (Qiagen) and 4 μ l of Oligofectamine, incubated for 48 h at 37°C, 5% CO₂, and then harvested and loaded in Boyden chambers. Transfection efficiency (nearly 90%) and functional specificity were monitored with the RNAi starter kit by using Alexa Fluor 488 labeled nonsilencing siRNA (Qiagen). uPAR silencing was assessed by Western-blot analysis with uPAR-specific antibodies and RT-PCR.

Reverse-polymerase chain reaction

Total cellular RNA was isolated by lysing cells in TRIzol Solution according to the supplier's protocol. RNA was precipitated and quantitated by spectroscopy. Total RNA (5 μ g) was reversely transcribed with random hexamer primers and 200 U of M-MLV reverse transcriptase. Then, 1 μ l of reversely transcribed DNA was amplified using FPRL2 specific 5' sense (AGTTGCTCCACAGGAATC CA) and 3' antisense (GCCAATAATGAAGTGGAGGA TGAGA) primers. PCR was performed in a thermocycler

for 40 cycles at 61°C. The reaction products were analyzed by electrophoresis in 1% agarose gel containing ethidium bromide, followed by photography under ultraviolet illumination.

Lipid rafts analysis

Cells were harvested by 2 mM EDTA-PBS and resuspended in $\text{Ca}^{2+}/\text{Mg}^{2+}$ -containing PBS. Washed cells (1×10^6) were plated in 35-mm plates coated with 10 $\mu\text{g}/\text{ml}$ of CG or VN and incubated for 1 h at 37°C. Cells were then lysed in lysis buffer (20 mM MOPS, 0.15 M NaCl, 1% Triton-X 100 and protease inhibitors) for 30 min at 4°C. The protein content was measured by a colorimetric assay (Bio-Rad) and 2 mg of protein was diluted to 1 ml, mixed with 1 ml of 80% sucrose in MOPS and placed at the bottom of a centrifuge tube. The samples were overlaid with 4 ml of 30%, 2 ml of 5%, 4 ml of 0% sucrose in MOPS and centrifuged at 39,000 rpm for 17 h using a SW41Ti rotor in a Beckman L7-55 ultracentrifuge at 4°C. After centrifugation, the top 4 ml was removed and the remaining 8 ml was harvested as 1 ml fractions. Equal volumes (60 μl) of each fraction were analyzed by Western blot.

Western-blot analysis

Samples were electrophoresed in 10% SDS-PAGE and transferred onto a PVDF filter. The membrane was blocked with 5% nonfat dry milk and probed with 1 $\mu\text{g}/\text{ml}$ of anti-uPAR, anti-integrin, anti-caveolin or anti-CXCR4 polyclonal antibodies, or with 2 $\mu\text{g}/\text{ml}$ of the anti-uPAR₈₄₋₉₅ polyclonal antibody. Finally, washed filters were incubated with horseradish peroxidase-conjugated secondary antibodies and detected by ECL.

Analysis of ERK 1/2 activation

Transfected cells were serum starved for 20 h, harvested by 2 mM EDTA-PBS and plated in wells pre-coated with 10 $\mu\text{g}/\text{ml}$ of CG or VN (10^6 cells/35 mm well) at 37°C, 5% CO_2 . At different time points, cells were lysed in 1% Triton X-100/PBS in the presence of protease and phosphatase inhibitors and the protein content was measured by a colorimetric assay. 30 μg of protein was electrophoresed in 12% SDS-PAGE and transferred to a PVDF membrane. The membrane was blocked with 5% nonfat dry milk and probed with 1 $\mu\text{g}/\text{ml}$ rabbit anti-phospho-ERK 1/2 and, then, with mouse anti-ERK 2 (as a loading control) antibodies. Finally, washed filters were incubated with horseradish peroxidase-conjugated anti-rabbit or anti-mouse antibodies; specific bands were detected by ECL.

Adhesion assay

Flat-bottom 96-well microtiter plates were coated with 10 $\mu\text{g}/\text{ml}$ of laminin, vitronectin, fibronectin, collagen or 1% heat-denatured BSA-PBS as a negative control, and incubated overnight at 4°C. The plates were then blocked 1 h at room temperature with 1% heat-denatured BSA-PBS. Cells were harvested by 2 mM EDTA-PBS and resuspended in $\text{Ca}^{2+}/\text{Mg}^{2+}$ -containing PBS. 10^5 cells were plated in each coated well and incubated for 1 h at 37°C. Then, wells were washed and attached cells were fixed with 3% paraformaldehyde in PBS for 10 min and then incubated with 2% methanol for 10 min. The cells were finally stained for 10 min with 0.5% crystal violet in 20% methanol. Stain was eluted by 0.1 M sodium citrate in 50% ethanol, pH 4.2, and the absorbance at 540 nm was measured with a spectrophotometer.

Statistical analysis

Differences between groups were evaluated by Student's *t* test using PRISM software (GraphPad, San Diego, CA). $p \leq 0.05$ was considered statistically significant.

Results

HEK-293 cells transfected with uPAR and CXCR4 cDNAs express both receptors which colocalize on their surface

To investigate whether the cell-surface uPAR can interfere with CXCR4 activity, uPAR- and CXCR4-negative HEK-293 cells were transfected with a cDNA coding for CXCR4, with cDNAs coding for uPAR and CXCR4, or with both the empty vectors, as negative controls; the corresponding transfected cells were named CXCR4-293, CXCR4/uPAR-293, V-293. Flow cytometry analysis with anti-uPAR and anti-CXCR4 antibodies showed a high expression of uPAR in uPAR-transfected cells and a moderate but comparable expression of CXCR4 on the cell surface of both uPAR-negative and uPAR-expressing cells (Fig. 1a). uPAR expressed by CXCR4/uPAR-293 cells was mostly in the full-length form, as shown by Western-blot analysis of CXCR4/uPAR-293 cell lysates with uPAR-specific antibodies (Fig. 1b).

Analysis by confocal microscopy of CXCR4/uPAR-293 cells further confirmed cell-surface expression of both receptors and showed CXCR4 colocalization with uPAR, which increased following SDF1 stimulation (Fig. 2). Accordingly with previous reports [26], uPAR-transfected 293 cells showed formation of extensive lamellipodia. Interestingly, uPAR localized both at the peripheral lamellipodia and at the more internal "lamella proper" of

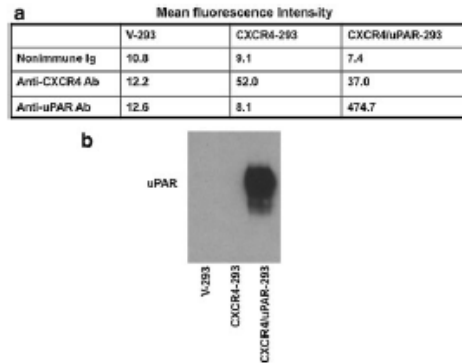
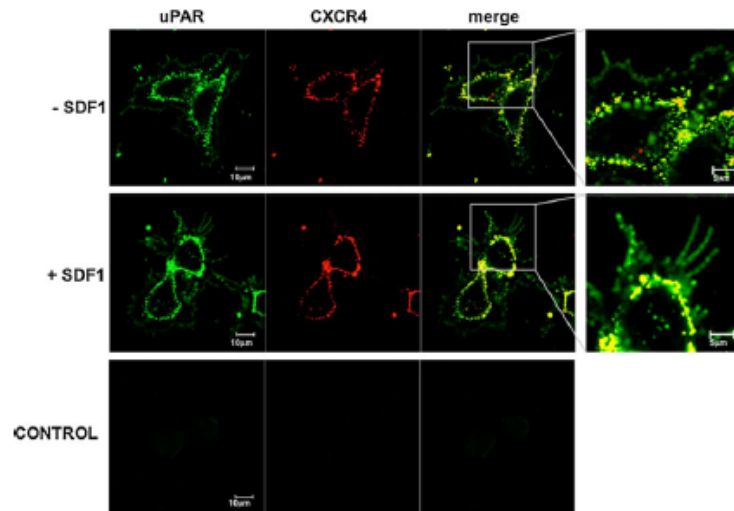


Fig. 1 uPAR and CXCR4 are expressed by transfected HEK-293 cells. **a** HEK-293 cells were transfected with CXCR4 cDNA (CXCR4-293), with uPAR and CXCR4 cDNAs (CXCR4/uPAR-293), or with empty vectors (V-293). Transfected cells were analyzed by flow cytometry with anti-CXCR4 antibodies, anti-uPAR antibodies or nonimmune immunoglobulins (Ig). **b** V-293, CXCR4-293 and CXCR4/uPAR-293 cells were lysed in 1% TRITON X-100 and 5 µg of proteins were analyzed by Western blot with uPAR-specific antibodies. uPAR, expressed only in CXCR4/uPAR-293 cells, was mainly in the full-length form

the leading edge of spreading cells [26], whereas CXCR4 colocalized with uPAR only at the “lamella proper”. SDF1 stimulation increased uPAR and CXCR4 focusing in dots at the “lamella proper”, likely corresponding to focal complexes [27].

Fig. 2 uPAR and CXCR4 colocalize on the surface of transfected HEK-293 cells. HEK-293 cells transfected with CXCR4 and uPAR cDNAs (CXCR4/uPAR-293) were grown on glass slides and stimulated with SDF1 or buffer for 1 h. Then cells were incubated with the mouse uPAR-specific antibody (green) and the rabbit CXCR4-specific antibody (red), and analyzed by confocal microscopy. SDF1-treated cells, incubated with nonimmune Ig and secondary antibodies, were shown as control. Scale bar 10 µm



These results demonstrate that CXCR4 and uPAR are expressed in transfected cells and colocalize on the cell surface, thus supporting the possibility of a functional interaction of these two receptors.

uPAR expression regulates SDF1-induced cell migration on VN and CG

In order to elucidate the potential influence of cell-surface uPAR in CXCR4 activity, we examined the capability of transfected cells to migrate toward SDF1, the CXCR4 ligand, on different ECM components. Firstly, the baseline migration of transfected cells on ECM components was assessed. Transfected cells were plated on filters coated with fibronectin (FN), laminin (LM), collagen (CG) or vitronectin (VN), and allowed to migrate in the absence of chemoattractants. The assay showed that the expression of both receptors does not affect the baseline migration of HEK-293 cells on specific substrates (Fig. 3a).

Then, transfected cells were allowed to migrate toward SDF1 (Fig. 3b). CXCR4-293 and CXCR4/uPAR-293 cells migrated with similar efficiency on FN and LM; thus, both CXCR4- and CXCR4/uPAR-293 cells express a functional CXCR4 on their surface. Interestingly, transfected cells behaved differently on the other two substrates. In fact, CXCR4-293 cells migrated efficiently toward SDF1 on CG, whereas they were unable to migrate on VN; conversely, CXCR4/uPAR-293 cells migrated efficiently on VN and very poorly on CG.

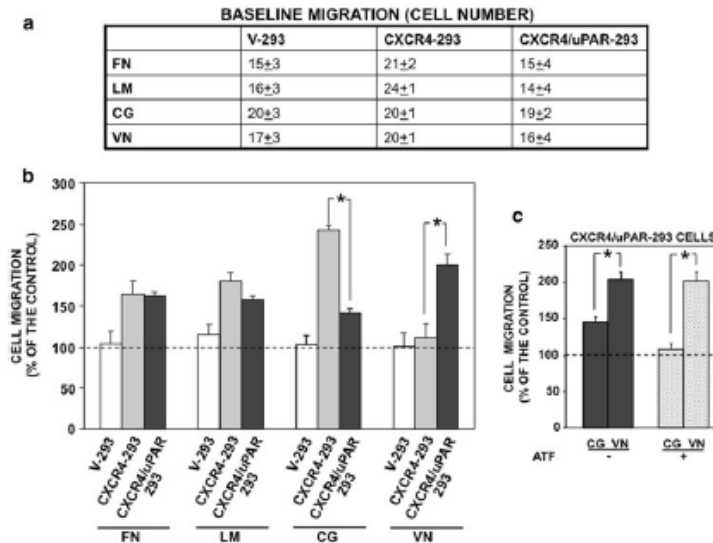


Fig. 3 uPAR expression affects SDF1-induced cell migration on VN and CG. **a** HEK-293 cells transfected with CXCR4 cDNA (CXCR4-293), uPAR and CXCR4 cDNAs, (CXCR4/uPAR-293) or empty vectors (V-293), were plated in Boyden chambers on filters coated with fibronectin (FN), laminin (LM), collagen (CG) or vitronectin (VN), and allowed to migrate in the absence of chemoattractants. The values are the mean \pm SD of three experiments performed in triplicate. **b** Transfected cells were plated in Boyden chambers and allowed to migrate toward 100 ng/ml SDF1 on filters coated with FN, LM, CG, or VN. 100% values represent cell migration in the absence

of chemoattractants. The values are the mean \pm SD of three experiments performed in triplicate. * $p \leq 0.05$ as determined by Student's *t* test. **c** CXCR4/uPAR-293 cells were plated in Boyden chambers and allowed to migrate toward 100 ng/ml SDF1 on filters coated with CG or VN, in the presence or in the absence of 10 nM of the aminoterminal fragment of uPA (ATF). ATF was added to both upper and lower compartments of the Boyden chamber. 100% values represent cell migration in the absence of chemoattractants. The values are the mean \pm SD of three experiments. * $p \leq 0.05$ as determined by Student's *t* test

Control cells, which do not express uPAR and CXCR4, did not migrate to SDF1 on all tested ECM components, as expected.

The observed effect of uPAR expression on cell migration toward SDF1 on CG and VN was due to the contemporaneous coexpression of uPAR and CXCR4, since we previously showed that the same HEK-293 cells used in the present report as recipient cells, transfected only with uPAR cDNA, migrated with similar efficiency on CG and VN toward different ligands [14].

HEK-293 cells do not produce uPA [28] which, upon binding to uPAR through its aminoterminal fragment (ATF), is able to increase uPAR interactions with VN and integrins, likely by promoting the active conformation of uPAR [9, 29]. We then investigated whether ATF could further influence SDF1-induced migration of CXCR4/uPAR-293 cells on VN and CG. ATF can contribute to uPAR effects on CXCR4 activity, further decreasing migration on CG (Fig. 3c).

Thus, uPAR expression does not affect SDF1-induced cell migration on LM and FN, whereas it strongly impairs migration on CG and allows migration on VN.

uPAR effects on CXCR4 activity are mediated by the uPAR₈₄₋₉₅ region

uPAR involvement in the regulation of CXCR4 activity on VN and CG was confirmed by chemotaxis assays performed in the presence of an anti-uPAR polyclonal antibody. In fact, the anti-uPAR antibody reversed CXCR4/uPAR-293 cell capability to migrate on these specific ECM components, impairing migration on VN and restoring migration on CG (Fig. 4a), thus inducing the same behavior of uPAR-negative CXCR4-293 cells (see Fig. 3b).

Then, we investigated the effect of a polyclonal antibody directed to the uPAR₈₄₋₉₅ region, which contains the binding sequence for fMLP receptors (residues

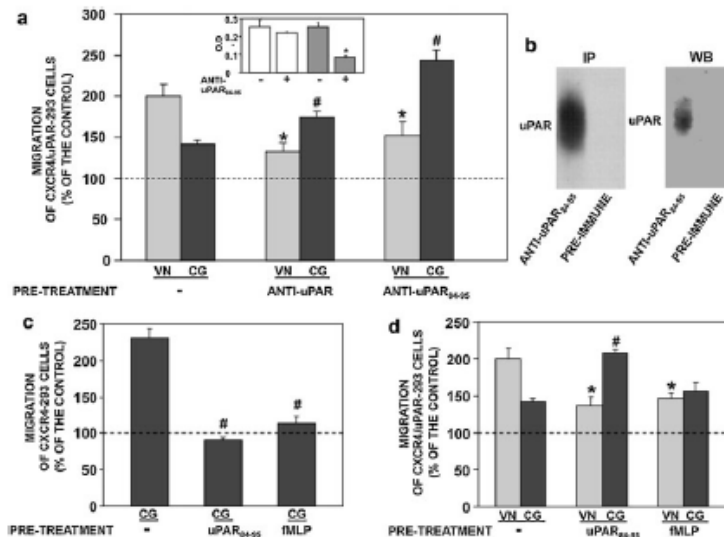


Fig. 4 uPAR effects on SDF1-induced migration involve the uPAR₈₄₋₉₅ epitope and fMLP-receptors. **a** CXCR4/uPAR-293 cells were incubated with nonimmune immunoglobulins (-), anti-uPAR antibodies or anti-uPAR₈₄₋₉₅ antibodies, plated in Boyden chambers and allowed to migrate toward 100 ng/ml SDF1 on filters coated with collagen (CG) and vitronectin (VN). 100% values represent cell migration in the absence of chemoattractants. The values are the mean \pm SD of three experiments performed in triplicate. * $p \leq 0.05$, as determined by Student's *t* test, compared to migration on VN of cells treated with nonimmune Ig. # $p \leq 0.05$, as determined by Student's *t* test, compared to migration on CG of cells treated with nonimmune Ig. *Inset* CXCR4/uPAR-293 cells were plated on VN-coated wells in the presence of 5 μ g/ml of nonimmune immunoglobulins (-) or the anti-uPAR₈₄₋₉₅ polyclonal antibody (*white columns*) or of 50 μ g/ml of nonimmune immunoglobulins (-) or the anti-uPAR₈₄₋₉₅ polyclonal antibody (*grey columns*). The attached cells were fixed and stained with crystal violet. The stain was eluted, and the absorbance at 540 nm was measured with a spectrophotometer. The values represent the means \pm SD of three experiments performed in triplicate. * $p \leq 0.05$, as determined by Student's *t* test. **b** Characterization of the anti-uPAR₈₄₋₉₅ polyclonal antibody: cell-surface

proteins of uPAR-transfected 293 cells were biotinylated; cells were lysed and 500 μ g of proteins were immunoprecipitated (IP) with 10 μ g/ml of the anti-uPAR₈₄₋₉₅ polyclonal antibody or pre-immune immunoglobulins (*left*). uPAR-293 cells were lysed in TRITON X-100 and 5 μ g of proteins were analyzed by Western blot (WB) with 10 μ g/ml of the anti-uPAR₈₄₋₉₅ polyclonal antibody (*right*). **c** CXCR4-293 cells were pre-incubated with buffer (-), 100 nM uPAR₈₄₋₉₅ peptide or 100 nM fMLP, plated in Boyden chambers and allowed to migrate toward 100 ng/ml SDF1 on CG-coated filters. 100% values represent cell migration in the absence of chemoattractants. The values are the mean \pm SD of three experiments performed in triplicate. * $p \leq 0.05$, as determined by Student's *t* test, compared to migration on CG of untreated cells. **d** CXCR4/uPAR-293 cells were pre-incubated with buffer (-), 100 nM uPAR₈₄₋₉₅ peptide or 100 nM fMLP, plated in Boyden chambers and allowed to migrate toward 100 ng/ml SDF1 on filters coated with CG or VN. 100% values represent cell migration in the absence of chemoattractants. The values are the mean \pm SD of three experiments performed in triplicate. * $p \leq 0.05$, as determined by Student's *t* test, compared to migration on VN of untreated cells. # $p \leq 0.05$, as determined by Student's *t* test, compared to migration on CG of untreated cells

88-92) [13, 16]. This specific antibody efficiently recognizes uPAR in Western blot and immunoprecipitation (Fig. 4b). Interestingly, the anti-uPAR₈₄₋₉₅ antibody induced the same effect of the anti-uPAR polyclonal antibody in a more pronounced manner, thus suggesting the involvement of this specific uPAR epitope in the regulation of CXCR4 activity (Fig. 4a). However, since the uPAR₈₄₋₉₅ region also contains two of the five residues implicated in uPAR binding to VN, i.e., Arg(91) and Tyr(92) [28, 30], we assessed whether the observed

effect of the anti-uPAR₈₄₋₉₅ polyclonal antibody on the migration of CXCR4/uPAR-293 cells could be due to the impairment of uPAR-VN interaction. A total of 5 μ g/ml of the anti-uPAR₈₄₋₉₅ antibody, able to impair CXCR4/uPAR-293 cell migration on VN and to restore their migration on CG, did not affect CXCR4/uPAR 293 cell adhesion to plastic-bound VN; an higher antibody concentration (50 μ g/ml), used as a positive control, impaired CXCR4/uPAR 293 cell adhesion to VN, as expected (Fig. 4a, inset).

These results suggest that the uPAR₈₄₋₉₅ region is implicated in uPAR-dependent regulation of CXCR4 activity likely through its interaction with fMLP-Rs.

uPAR effects on SDF1-induced migration involve fMLP-receptors

The uPAR₈₄₋₉₅ epitope, involved in the regulation of CXCR4 activity, interacts with fMLP-Rs [13, 14]. HEK-293 cells express the high-affinity fMLP receptor (FPR), whereas they do not express the low affinity receptor (FPRL-1) [14]; therefore, we explored the involvement of FPR in the uPAR-dependent regulation of CXCR4 activity. FPR can be desensitized by treating cells with its ligands before migration [31]. fMLP and the soluble uPAR-derived peptide, covering the uPAR₈₄₋₉₅ region (uPAR₈₄₋₉₅), are ligands of fMLP-Rs, including FPR [13, 14]. Thus, we firstly examined the involvement of FPR in the migration on CG of CXCR4-293 cells, which do not express uPAR, desensitizing FPR. CXCR4-293 cells, following treatment with uPAR₈₄₋₉₅ peptide or fMLP, were unable to migrate toward SDF1 on CG (Fig. 4c), suggesting that SDF1-induced migration on CG of CXCR4-293 cells requires FPR activity, or, alternatively, that fMLP induces heterologous desensitization [31] of CXCR4, as shown in other cell systems [19–22]. Migration on VN, following FPR desensitization, was not performed since CXCR4-293 cells do not migrate on VN (see Fig. 3b).

We then examined FPR involvement in the migration on CG and VN of CXCR4/uPAR-293 cells (Fig. 4d). Pre-treatment of CXCR4/uPAR-293 cells with the uPAR₈₄₋₉₅ peptide impaired migration on VN and restored migration on CG (Fig. 4d), fully neutralizing the effect of uPAR expression, similarly to the anti-uPAR₈₄₋₉₅ antibody (Fig. 4a). fMLP cell-treatment reduced CXCR4/uPAR-293 cell migration on VN, as the uPAR₈₄₋₉₅ peptide, whereas it did not significantly restore migration on CG. These results prompted us to assess whether both fMLP and the uPAR₈₄₋₉₅ peptide target FPR in CXCR4/uPAR-293 cells. To this end, we evaluated the effect of uPAR₈₄₋₉₅ and fMLP on agonist-dependent FPR internalization [32]. The exposure of CXCR4/uPAR-293 cells to the fluorescent FPR-agonist *N*-formyl-Nle-Leu-Phe-Nle-Tyr-Lys at 37°C induced FPR internalization, as indicated by punctuate green fluorescent intra-cytoplasmic spots (Fig. 5a, left panels), according with previous reports [33]. The internalization of the fluorescent FPR-agonist was prevented by cell pre-incubation with the uPAR₈₄₋₉₅ peptide (Fig. 5a, right panels). These results demonstrate that both ligands specifically bind FPR in CXCR4/uPAR-293 cells, even they show a different effect on the SDF1-induced migration on CG.

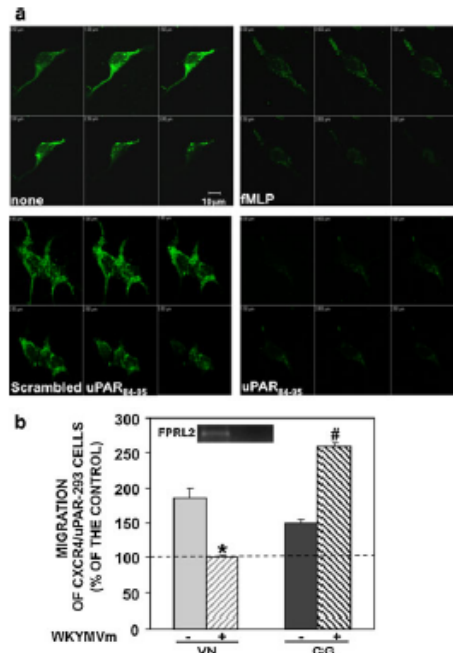


Fig. 5 uPAR₈₄₋₉₅ peptide and fMLP prevent agonist-FPR interaction. All fMLP-receptors expressed by HEK-293 are involved in uPAR effects on SDF1-induced migration. **a** Representative confocal images of CXCR4/uPAR-293 cells incubated with buffer (none), 100 nM fMLP, 100 nM uPAR₈₄₋₉₅ peptide or 100 nM scrambled peptide for 30 min at 37°C and exposed for further 30 min at 37°C to 10 nM *N*-formyl-Nle-Leu-Phe-Nle-Tyr-Lys-fluorescein. Z-series images represent focal planes corresponding to 0.5 μ m vertical interval. Original magnification 630 \times . Scale bar 10 μ m. **b** CXCR4/uPAR-293 cells were pre-incubated with buffer (-) or 5 nM WKYMVm peptide, plated in Boyden chambers and allowed to migrate toward 100 ng/ml SDF1 on filters coated with collagen (CG) or vitronectin (VN). 100% values represent cell migration in the absence of chemoattractants. The values are the mean \pm SD of three experiments. * $p \leq 0.05$, as determined by Student's *t* test. Inset 5 μ g of total RNA from CXCR4/uPAR-293 cells was reverse transcribed and amplified using FPRL2-specific primers. The reaction products were analyzed by electrophoresis and stained with ethidium bromide, followed by photography under ultraviolet illumination

Then, we reasoned that fMLP is able to bind only two among the three fMLP receptors, i.e., FPR and FPRL1, while it does not bind FPRL2; vice versa, the uPAR₈₄₋₉₅ peptide interacts with all three fMLP receptors, including FPRL2. Thus, the uPAR₈₄₋₉₅ peptide could totally neutralize uPAR effects by targeting also FPRL2, beside FPR, unlike fMLP. Therefore, we assessed FPRL2 expression in CXCR4/uPAR 293-cell (Fig. 5b, inset) and evaluated

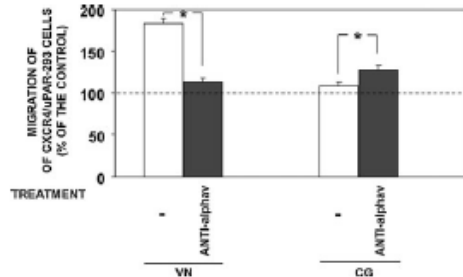


Fig. 6 uPAR effects on SDF1-induced migration involve specific integrins. CXCR4/uPAR-293 cells were incubated with nonimmune Ig (-) or an anti-alpha-v monoclonal antibody, plated in Boyden chambers and allowed to migrate toward 100 ng/ml SDF1 on filters coated with collagen (CG) or vitronectin (VN). 100% values represent cell migration in the absence of chemoattractants. The values are the mean \pm SD of three experiments performed in triplicate. * $p \leq 0.05$, as determined by Student's *t* test

CXCR4/uPAR-293 cell migration on CG and VN, following treatment with the synthetic peptide WKYMVm, which is a ligand for all three fMLP receptors [15]. Pre-incubation of CXCR4/uPAR-293 cells with the WKYMVm peptide completely neutralized the effect of uPAR on CXCR4-mediated migration, impairing CXCR4/uPAR-293 cell migration on VN and restoring their migration on CG, similarly to the uPAR₈₄₋₉₅ peptide (Fig. 5b).

All together, these results indicate that the uPAR-dependent regulation of CXCR4 activity involves all fMLP receptors expressed by HEK-293 cells.

uPAR effects on SDF1-induced migration involve specific integrins

uPAR is a GPI-anchored protein, and requires functional partners provided with cytosolic domains for signal transduction. Integrins interact with uPAR and have been proposed as the best candidates to mediate uPAR signaling [34, 35]. We then also explored the role of alpha-v integrins, which are expressed in HEK-293 cells and are involved in uPAR-related cell signals [36, 37], in uPAR-dependent regulation of CXCR4 activity. CXCR4/uPAR-293 cells were allowed to migrate toward SDF1 on VN or CG in the presence of nonimmune Ig or an anti-alpha-v monoclonal antibody. Specific antibodies significantly reduced migration of CXCR4/uPAR-293 cells on VN, and moderately restored migration on CG (Fig. 6).

These results demonstrate that also integrins are involved in uPAR-related activities enabling CXCR4/uPAR-293 cells to migrate on VN and impairing migration on CG.

uPAR expression down-regulates adhesion of CXCR4-transfected cells

We then investigated whether uPAR expression influences also the stable adhesion to ECM of CXCR4-expressing

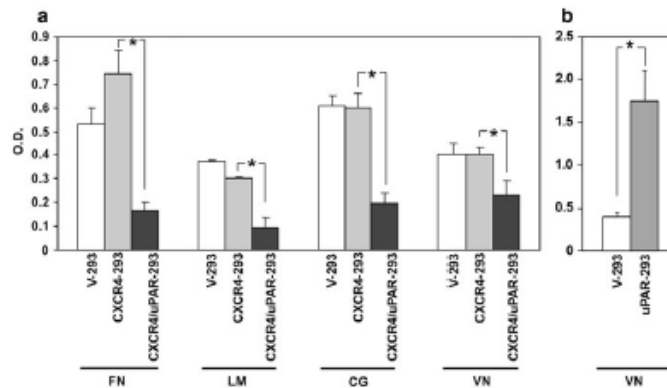


Fig. 7 uPAR expression down-regulates the adhesion of CXCR4-transfected cells to ECM components. **a** CXCR4-293, CXCR4/uPAR-293 or control cells (V-293) were plated on FN-, LM-, CG-, or VN-coated wells. The attached cells were fixed and stained with crystal violet. The stain was eluted, and the absorbance at 540 nm was measured by a spectrophotometer. The values represent the mean \pm SD of six experiments performed in triplicate. * $p \leq 0.05$,

as determined by Student's *t* test. **b** HEK-293 cells transfected with uPAR cDNA (uPAR-293) or control cells transfected with the empty vector (V-293) were plated on VN-coated wells. The attached cells were fixed and stained with crystal violet. The stain was eluted, and the absorbance at 540 nm was measured by a spectrophotometer. The values represent the mean \pm SD of three experiments performed in triplicate. * $p \leq 0.05$, as determined by Student's *t* test

cells. The adherence of V-293 control cells, CXCR4-293 and CXCR4/uPAR-293 cells to different components of the ECM was examined (Fig. 7a). Transfected cells were plated on FN, LM, CG, and VN coated wells. Adherent cells were stained by crystal violet and the absorbance of eluted stain was measured. CXCR4-293 cells adhered efficiently to all substrates, as well as control cells, even though no significant variations were observed in their adhesion to FN and LM. uPAR co-expression down-regulated cell adhesion to all substrates, including VN. CXCR4/uPAR-293 cell behavior on VN was unexpected, since uPAR expression had been previously shown to up-regulate HEK-293 cell adhesion to VN [38]; increased adhesion of HEK-293 cells upon transfection with only uPAR cDNA was confirmed in control experiments (Fig. 7b).

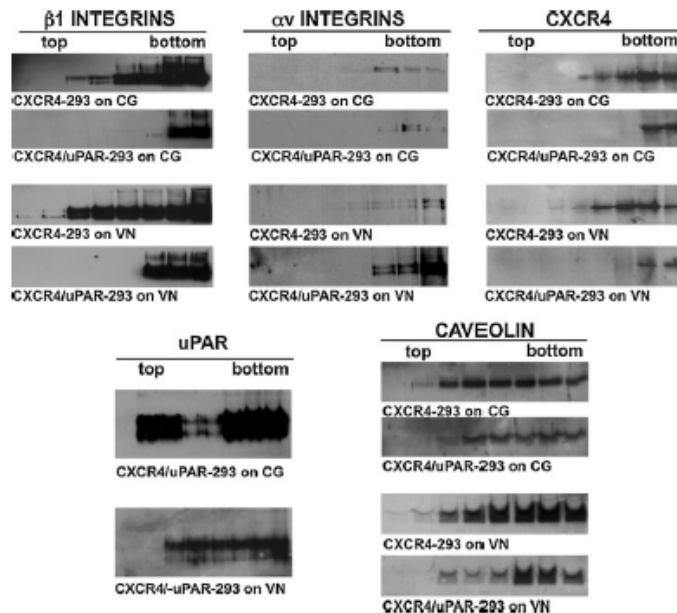
uPAR expression reduces integrin association to lipid rafts in CXCR4-expressing cells

uPAR association to lipid rafts has been previously shown [7]. Lipid rafts are cholesterol-rich microdomains of cell membrane that represent anchoring platforms for specific cell-signaling mediators and can be associated to active integrins [8, 39]. Thus, the effect of uPAR expression on the partitioning of integrins to lipid rafts has been examined.

Protein association to lipid rafts is evaluated by ultracentrifugation of cell lysates in a sucrose gradient, in which proteins excluded from lipid rafts remain in the bottom, whereas proteins associated to lipid rafts tend to float to the top, together with lipids. Lysates of transfected cells plated on CG and VN have been loaded on a sucrose gradient and ultracentrifuged. Harvested fractions have been analyzed by Western blot with antibodies directed to beta1 or alpha-v integrins, CXCR4, and uPAR or caveolin as floating controls [7, 40] (Fig. 8). Beta1 distribution was analyzed to investigate the effect of uPAR on integrins with different specificities, since beta1 associates to a wide variety of alpha chains; alpha-v partitioning was examined because this VN-specific alpha chain is a signaling partner for uPAR [37].

In lysates from uPAR-negative CXCR4-293 cells plated on CG and VN, beta1 integrins were present both in the bottom of the gradient, which contains the solubilized non-raft membranes, and in the upper fractions, containing the detergent-resistant lipid rafts. By contrast, in lysates from CXCR4/uPAR-293 cells plated on the same substrates, beta1 integrins were totally confined to the bottom of the gradient, thus associated to non-raft membranes (Fig. 8, upper). Alpha-v integrins appeared associated to non-lipid fractions (bottom fractions) in both CXCR4- and CXCR4/uPAR-293 cells plated on CG; by contrast, they tended to

Fig. 8 uPAR expression affects integrin association to lipid rafts. CXCR4-293 and CXCR4/uPAR-293 cells were plated on CG- or VN-coated wells, incubated for 1 h at 37°C and lysed in buffer containing 1% Triton X-100. Cell lysates were subjected to sucrose density gradient ultracentrifugation. After centrifugation, 8 ml was harvested as 1-ml fractions. Equal volumes of each fraction were analyzed by Western blot with anti-beta1 or anti-alpha-v integrin antibodies (upper panels) or with anti-CXCR4 antibodies (upper panels) or with anti-uPAR or anti-caveolin antibodies (lower panels)



float with lipid rafts in CXCR4-293 cells and to remain in the bottom fractions in CXCR4/uPAR-293 cells plated on VN, similarly to beta1 integrins (Fig. 8, upper). The analysis of other integrins, such as beta3, alpha5, and alpha3, showed a partitioning pattern very similar to that of beta1 integrins (not shown).

CXCR4 partitioned to lipid and non-lipid fractions in uPAR-negative CXCR4-293 cells plated on both CG and VN, as reported in other cells types [41], whereas it was confined, as integrins, in non-lipid fractions in uPAR-expressing cells (Fig. 8, upper).

uPAR, expressed only in CXCR4/uPAR 293 cells, was found both in the bottom of the gradient, and in the top fractions, as previously shown in the same cells transfected only with uPAR [7]. Caveolin, which associates to lipid-rafts [40], was used as a control (Fig. 8, lower).

All together, these results show that uPAR, partitioned to both lipid raft and non lipid raft fractions, affects integrin and CXCR4 association to lipid rafts, confining them in non-raft membranes.

uPAR expression affects ERK 1/2 activation in CXCR4-transfected cells

Integrin confinement in non lipid-raft fractions could suggest modifications in their signaling pathways [39]. Integrin-dependent signaling pathways can converge on various mediators, including extracellular regulated kinases (ERK1/2) [42]. Thus, we explored the possibility that the affected partition of integrins to lipid rafts, induced by uPAR co-expression in CXCR4 transfected cells, could coincide with a modification of integrin-mediated signaling.

CXCR4-293 and CXCR4/uPAR-293 cells were serum-starved, plated on CG or VN, harvested at the indicated times and lysed. Western-blot analysis with anti-phospho-ERKs 1/2 antibodies showed ERK1/2 activation in CXCR4-293 cells plated both on CG and VN, even if at different incubation times (Fig. 9, left upper and lower panels, respectively). By contrast, ERK1/2 activation was

not detected in CXCR4/uPAR 293 cells plated on the same substrates (Fig. 9, right panels), suggesting a modification of ECM-dependent signaling following uPAR expression in CXCR4-expressing cells.

uPAR regulates SDF1-induced migration in tumor cells

uPAR and CXCR4 are up-regulated in several types of tumor [5, 9]; thus, the interference of uPAR in CXCR4 activity was examined also in tumor cells that constitutively express both receptors. PC3 prostate carcinoma cells express uPA, uPAR, and CXCR4 [43, 44], thus, their migration to SDF1 on CG and VN, in the presence or in the absence of the anti-uPAR₈₄₋₉₅ polyclonal antibody, was examined. The results showed that PC3 cells migrated efficiently on VN and poorly on CG in a SDF1 gradient; the anti-uPAR₈₄₋₉₅ polyclonal antibody and the uPAR₈₄₋₉₅ peptide, ligand of all three fMLP receptors, reduced their migration on VN and allowed a significant migration on CG (Fig. 10a, b), as for CXCR4/uPAR-transfected 293 cells (Fig. 4a).

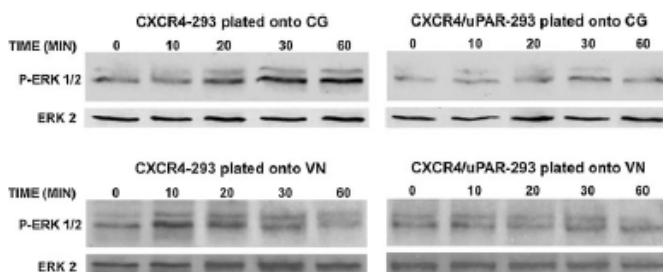
To further support these results, uPAR expression in PC3 cells was silenced by transfection with a specific siRNA. Migration toward SDF1 of PC3 cells transfected with a uPAR-specific siRNA or a control siRNA was examined, showing that uPAR silencing in PC3 cells induced the same effect of the anti-uPAR₈₄₋₉₅ polyclonal antibody and of the uPAR₈₄₋₉₅ peptide (Fig. 10c, left). uPAR silencing was assessed by Western-blot analysis of transfected cell lysates (Fig. 10c, right) and real-time PCR analysis (not shown).

These results confirm in tumor cells the interference of uPAR in CXCR4 activity observed in transfected cells.

Discussion

Chemokine gradients are central to direct the movement of cells in many normal and pathologic processes. We previously found that a soluble form of uPAR, exposing the

Fig. 9 uPAR expression affects ECM signaling in CXCR4 expressing cells. CXCR4-293 (left) and CXCR4/uPAR-293 (right) cells were serum-starved and plated on collagen (CG) (upper panels) or vitronectin (VN) (lower panels). The cells were harvested at the indicated times and lysed for Western-blot analysis with anti-phospho-ERKs and anti-ERK 2 (as a loading control) antibodies



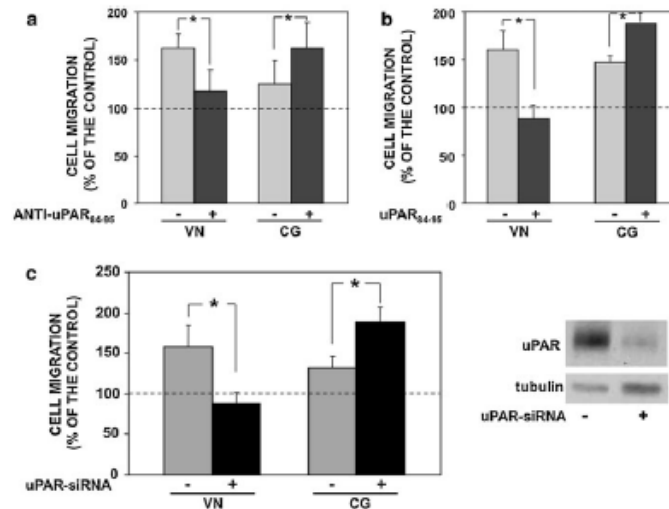


Fig. 10 uPAR expression regulates SDF1-induced migration in tumor cells. **a** PC3 cells were pre-incubated with nonimmune Ig (-) or the polyclonal anti-uPAR₈₄₋₉₅ antibody, plated in Boyden chambers and allowed to migrate toward 100 ng/ml SDF1 on filters coated with CG or VN (left). 100% values represent cell migration in the absence of chemoattractants. The values are the mean \pm SD of three experiments performed in triplicate. * $p \leq 0.05$, as determined by Student's *t* test. uPAR silencing was assessed by Western-blot analysis of transfected cell lysates with uPAR-specific antibodies (right)

uPAR-specific siRNA (+) or a control siRNA (-). Transfected cells were plated in Boyden chambers and allowed to migrate toward 100 ng/ml SDF1 on filters coated with CG or VN (left). 100% values represent cell migration in the absence of chemoattractants. The values are the mean \pm SD of three experiments performed in triplicate. * $p \leq 0.05$, as determined by Student's *t* test. uPAR silencing was assessed by Western-blot analysis of transfected cell lysates with uPAR-specific antibodies (right)

chemotactically active SRSRY sequence (aa 88–92), inhibited migration of HSCs toward the SDF1 [17, 25]. On this basis, in the present report, we investigate whether the cell-surface uPAR could interfere with CXCR4 activity, thus playing a new role in chemokine-mediated cancer cell trafficking.

We transfected HEK-293 cells with CXCR4 or with both receptors and observed their colocalization on the cell surface. Then, transfected cells were analyzed in functional assays. We showed that CXCR4-transfected cells efficiently migrated to SDF1 on CG and were unable to migrate on VN. The co-expression of cell-surface uPAR, which is a VN receptor [28], allowed cell migration on VN, a component largely expressed in tumor-associated ECM [10, 11], whereas it strongly impaired migration on CG. Antibodies against α -v integrins, or cell pre-treatment with fMLP-receptor (fMLP-R) ligands [15], such as fMLP, the synthetic WKYMVm peptide, the soluble uPAR₈₄₋₉₅ peptide, impaired SDF1-induced migration on VN of CXCR4/uPAR-293 cells, strongly suggesting that α -v integrins and fMLP-receptors are likely uPAR partners in cell-signaling on VN. In fact, uPAR lacks the cytosolic

domain, thus it requires cell-surface partners to transduce signals inside the cell.

Interestingly, pre-treatment of CXCR4/uPAR-293 cells with fMLP, able to desensitize FPR and FPRL-1, only impaired CXCR4/uPAR-293 cell migration on VN, but was not able to restore their migration on CG, whereas soluble uPAR₈₄₋₉₅ and WKYMVm peptides, also targeting FPRL-2, completely restored migration on CG. This observation suggests that also uPAR capability to impair cell migration to SDF1 on CG depends on its interaction with fMLP-Rs, in particular with FPRL-2. Indeed, we previously demonstrated that, in human basophils, uPAR function is mostly mediated by its interaction with FPRL-1 and FPRL-2 [45].

Besides regulating SDF1-induced migration on specific ECM substrates, we also showed that uPAR expression significantly decreased the adherence of CXCR4-expressing cells to various components of the ECM. The decrease in HEK-293 cell adhesion to CG, FN and LM, following uPAR expression, was in agreement with previous results obtained with HEK-293 cells transfected only with the uPAR cDNA [14, 38], although, in other cell types, uPAR up-regulation induces activation of FN-specific integrins

[46]. On the contrary, CXCR4/uPAR-293 cell behavior on VN was unexpected, since uPAR expression had been previously shown to up-regulate HEK-293 cell adhesion to VN [38], thus suggesting a reciprocal interference between uPAR and CXCR4. In agreement with cell-adhesion results, uPAR seems to saturate lipid rafts and to exclude integrins from these membrane microdomains, which would play a proactive function in clustering integrins and in the priming of cells for efficient ligand binding [47]. Integrin confinement in non lipid-raft fractions could suggest a modulation of their ligand-binding activity and, likely, modifications in their signaling pathways. In fact, we found that uPAR expression in CXCR4-expressing cells impairs ERK 1/2 activation induced by ECM components (Fig. 9). Thus, integrin confinement in non lipid-raft fractions and modifications in their signaling pathways could contribute to the impaired adhesion observed in CXCR4/uPAR transfected cells.

All together, our results demonstrate that the simultaneous expression of CXCR4 and uPAR influences the adhesive and migratory features of cells. In particular, cells become less adherent to ECM and, at the same time, acquire the capability to migrate toward SDF1 on VN. The mechanism involves both fMLP-receptors and alpha-v integrins, previously proposed as uPAR partners in the activation of cell-signaling pathways. On this basis, we propose that uPAR functionally associates to a supramolecular complex including such molecules; the exclusion of fMLP-Rs or alpha-v integrins from the complex abolishes uPAR capability to regulate CXCR4 activity. The possibility that uPAR, fMLP-Rs, integrins and CXCR4 form a functional complex is based on previous literature. In fact, uPAR can interact, at least functionally, with FPR, through the SRSRY sequence [13, 14], and with integrins, through specific sequence in the D2 and the D3 domains [48, 49]. A cross-talk between CXCR4 and fMLP-Rs is suggested by fMLP capability to desensitize CXCR4 [20, 21], and, on the other hand, by the requirement of fMLP-Rs for the activity of specific chemokine receptors [22]; CXCR4 can regulate the activity of specific integrins and, in turn, its activity can be regulated by integrins [50].

We confirmed uPAR interference in CXCR4 activity in cells derived from prostate carcinomas, in which the expression of uPAR and CXCR4 and the importance of the CXCR4-SDF1 axis have been previously demonstrated [51, 52].

CXCR4 is up-regulated in a large number of common human cancers, such as those of breast, lung, prostate, colon, and in melanoma [2–5]. A variety of strategies have been used to target the CXCR4-SDF1 axis and few compounds are advancing into early stages of clinical development in oncology [53]. uPAR also is strongly up-regulated in various malignancies, including carcinomas [54]. The finding that

uPAR can exist also in soluble and cleaved forms and that can regulate the functions of various integrin families and the activity of growth factor and chemokine receptors suggested new potential roles for uPAR in cancer, beside the focusing of uPA proteolytic activity [55]. Several approaches have been proposed in cancer therapy to disrupt ligand-dependent and ligand-independent uPAR activities [56]. Recently, increased expression of fMLP-Rs in some cancers has been reported [24].

The simultaneous expression of CXCR4, fMLP-Rs, and uPAR, observed in various tumors, could thus reinforce a neoplastic phenotype, characterized by decreased adherence to physiologic ECM and by enhanced capability to migrate on VN, suggesting the uPAR-fMLP-Rs-CXCR4 cross-talk as a new molecular target in combating cancer.

Acknowledgments This work was supported by grants from the Ministero dell'Istruzione, dell'Università e della Ricerca (MIUR, PRIN 2007), from Associazione Italiana per la Ricerca sul Cancro (AIRC, IG 4714) and from Ministero Italiano della Salute-FSN2007.

References

- Murdoch C (2000) CXCR4: chemokine receptor extraordinaire. *Immunol Rev* 177:175–184
- Balkwill F (2004) The significance of cancer cell expression of the chemokine receptor CXCR4. *Semin Cancer Biol* 14:171–179
- Kucia M, Rea R, Miekus K, Wanzeck J, Wojakowski W, Janowska-Wieczorek A, Ratajczak J, Ratajczak MZ (2005) Trafficking of normal stem cells and metastasis of cancer stem cells involve similar mechanisms: pivotal role of the SDF-1-CXCR4 axis. *Stem Cells* 23:879–894
- Zlonik A (2006) Chemokines and cancer. *Int J Cancer* 119:2026–2029
- Burger JA, Kipps TJ (2006) CXCR4: a key receptor in the crosstalk between tumor cells and their microenvironment. *Blood* 107:1761–1767
- Irigoyen JP, Munoz-Canoves P, Montero L, Koziczak M, Nagamine Y (1999) The plasminogen activator system: biology and regulation. *Cell Mol Life Sci* 56:104–132
- Cunningham O, Andolfo A, Santovito ML, Iuzzolino L, Blasi F, Sidenius N (2003) Dimerization controls the lipid raft partitioning of uPAR/CD87 and regulates its biological functions. *EMBO J* 22:5994–6003
- Viola A, Gupta N (2007) Tether and trap: regulation of membrane-raft dynamics by actin-binding proteins. *Nat Rev Immunol* 7:889–896
- Ragno P (2006) The urokinase receptor: a ligand or a receptor? Story of a sociable molecule. *Cell Mol Life Sci* 63:1028–1037
- Felding-Habermann B, Cheresh DA (1993) Vitronectin and its receptors. *Curr Opin Cell Biol* 5:864–868
- Henry C, Moitessier N, Chapleur Y (2002) Vitronectin receptor alpha(V)beta(3) integrin antagonists: chemical and structural requirements for activity and selectivity. *Mini Rev Med Chem* 2:531–534
- Montuori N, Ragno P (2009) Multiple activities of a multifaceted receptor: roles of cleaved and soluble uPAR. *Front Biosci* 14:2494–2503
- Resnati M, Pallavicini I, Wang JM, Oppenheim J, Serhan CN, Romano M, Blasi F (2002) The fibrinolytic receptor for urokinase

- activates the G protein-coupled chemotactic receptor FPRL1/LXA4R. *Proc Natl Acad Sci USA* 99:1359–1364
14. Montuori N, Carriero MV, Salzano S, Rossi G, Ragno P (2002) The cleavage of the urokinase receptor regulates its multiple functions. *J Biol Chem* 277:46932–46939
 15. Le Y, Murphy PM, Wang JM (2002) Formyl-peptide receptors revisited. *Trends Immunol* 23:541–548
 16. Fazioli F, Resnati M, Sidenius N, Higashimoto Y, Appella E, Blasi F (1997) A urokinase-sensitive region of the human urokinase receptor is responsible for its chemotactic activity. *EMBO J* 16:7279–7286
 17. Selleri C, Montuori N, Ricci P, Visconte V, Carriero MV, Sidenius N, Serio B, Blasi F, Rotoli B, Rossi G, Ragno P (2005) Involvement of the urokinase-type plasminogen activator receptor in hematopoietic stem cell mobilization. *Blood* 105:2198–2205
 18. Gargiulo L, Longanesi-Cattani I, Bifulco K, Franco P, Raiola R, Campiglia P, Grieco P, Peluso G, Stoppelli MP, Carriero MV (2005) Cross-talk between fMLP and vitronectin receptors triggered by urokinase receptor-derived SRSRY peptide. *J Biol Chem* 280:25225–25232
 19. Furlan F, Orlando S, Laudanna C, Resnati M, Basso V, Blasi F, Mondino A (2004) The soluble D2D3(88–274) fragment of the urokinase receptor inhibits monocyte chemotaxis and integrin-dependent cell adhesion. *J Cell Sci* 117:2909–2916
 20. Li BQ, Wetzel MA, Mikovits JA, Henderson EE, Rogers TJ, Gong W, Le Y, Ruscetti FW, Wang JM (2001) The synthetic peptide WKYMVm attenuates the function of the chemokine receptors CCR5 and CXCR4 through activation of formyl peptide receptor-like 1. *Blood* 97:2941–2947
 21. Le Y, Shen W, Li B, Gong W, Dunlop NM, Wang JM (1999) A new insight into the role of “old” chemotactic peptide receptors FPR and FPRL1: down-regulation of chemokine receptors CCR5 and CXCR4. *Forum (Genova)* 9:299–314
 22. Svensson L, Redvall E, Johnsson M, Stenfeldt AL, Dahlgren C, Wennerås C (2009) Interplay between signaling via the formyl peptide receptor (FPR) and chemokine receptor 3 (CCR3) in human eosinophils. *J Leukoc Biol* 86:327–336
 23. Chigaev A, Waller A, Amit O, Halip L, Bologna CG, Sklar LA (2009) Real-time analysis of conformation-sensitive antibody binding provides new insights into integrin conformational regulation. *J Biol Chem* 284:14337–14346
 24. Huang J, Chen K, Gong W, Dunlop NM, Wang JM (2008) G-protein coupled chemoattractant receptors and cancer. *Front Biosci* 13:3352–3363
 25. Selleri C, Montuori N, Ricci P, Visconte V, Baiano A, Carriero MV, Rotoli B, Rossi G, Ragno P (2006) In vivo activity of the cleaved form of soluble urokinase receptor: a new hematopoietic stem/progenitor cell mobilizer. *Cancer Res* 66:10885–10890
 26. Madsen CD, Ferraris GM, Andolfo A, Cunningham O, Sidenius N (2007) uPAR-induced cell adhesion and migration: vitronectin provides the key. *J Cell Biol* 177:927–939
 27. Wolfenson H, Henis YI, Geiger B, Bershadsky AD (2009) The heel and toe of the cell's foot: a multifaceted approach for understanding the structure and dynamics of focal adhesions. *Cell Motil Cytoskeleton* 66:1017–1029
 28. Wei Y, Waltz DA, Rao N, Drummond RJ, Rosenberg S, Chapman HA (1994) Identification of the urokinase receptor as an adhesion receptor for vitronectin. *J Biol Chem* 269:32380–32388
 29. Yuan C, Huang M (2007) Does the urokinase receptor exist in a latent form? *Cell Mol Life Sci* 64:1033–1037
 30. Gårdsvoll H, Ploug M (2007) Mapping of the vitronectin-binding site on the urokinase receptor: involvement of a coherent receptor interface consisting of residues from both domain I and the flanking interdomain linker region. *J Biol Chem* 282:13561–13572
 31. Ali H, Richardson RM, Haribabu B, Snyderman R (1999) Chemoattractant receptor cross-desensitization. *J Biol Chem* 274:6027–6030
 32. Rabiet MJ, Huet E, Boulay F (2007) The N-formyl peptide receptors and the anaphylatoxin C5a receptors: an overview. *Biochimie* 89:1089–1106
 33. Bifulco K, Longanesi-Cattani I, Gargiulo L, Maglio O, Cataldi M, De Rosa M, Stoppelli MP, Pavone V, Carriero MV (2008) An urokinase receptor antagonist that inhibits cell migration by blocking the formyl peptide receptor. *FEBS Lett* 582:1141–1146
 34. Blasi F, Carmeliet P (2002) uPAR: a versatile signalling orchestrator. *Nat Rev Mol Cell Biol* 3:932–943
 35. Ossowski L, Aguirre-Ghiso JA (2000) Urokinase receptor and integrin partnership: coordination of signaling for cell adhesion, migration and growth. *Curr Opin Cell Biol* 12:613–620
 36. Franco P, Vocca I, Carriero MV, Alfano D, Cito L, Longanesi-Cattani I, Grieco P, Ossowski L, Stoppelli MP (2006) Activation of urokinase receptor by a novel interaction between the connecting peptide region of urokinase and alpha v beta 5 integrin. *J Cell Sci* 119:3424–3434
 37. Carriero MV, Del Vecchio S, Capozzoli M, Franco P, Fontana L, Zannetti A, Boti G, D'Aiuto G, Salvatore M, Stoppelli MP (1999) Urokinase receptor interacts with alpha(v)beta5 vitronectin receptor, promoting urokinase-dependent cell migration in breast cancer. *Cancer Res* 59:5307–5314
 38. Wei Y, Lukashev M, Simon DL, Bodary SC, Rosenberg S, Doyle MV, Chapman HA (1996) Regulation of integrin function by the urokinase receptor. *Science* 273:1551–1555
 39. Del Pozo MA (2004) Integrin signaling and lipid rafts. *Cell Cycle* 3:725–728
 40. Lajoie P, Goetz JG, Dennis JW, Nabi IR (2009) Lattices, rafts, and scaffolds: domain regulation of receptor signaling at the plasma membrane. *J Cell Biol* 185:381–385
 41. Nguyen DH, Taub D (2002) CXCR4 function requires membrane cholesterol: implications for HIV infection. *J Immunol* 168:4121–4126
 42. Harburger DS, Calderwood DA (2009) Integrin signalling at a glance. *J Cell Sci* 122:159–163
 43. Festuccia C, Dolo V, Guerra F, Violini S, Muzi P, Pavan A, Bologna M (1998) Plasminogen activator system modulates invasive capacity and proliferation in prostatic tumor cells. *Clin Exp Metastasis* 16:513–528
 44. Cannio R, Rennie PS, Blasi F (1991) A cell-type specific and enhancer-dependent silencer in the regulation of the expression of the human urokinase plasminogen activator gene. *Nucleic Acids Res* 19:2303–2308
 45. de Paulis A, Montuori N, Prevece N, Fiorentino I, Rossi FW, Visconte V, Rossi G, Marone G, Ragno P (2004) Urokinase induces basophil chemotaxis through a urokinase receptor epitope that is an endogenous ligand for formyl peptide receptor-like 1 and -like 2. *J Immunol* 173:5739–5748
 46. Aguirre Ghiso JA, Kovacki K, Ossowski L (1999) Tumor dormancy induced by downregulation of urokinase receptor in human carcinoma involves integrin and MAPK signaling. *J Cell Biol* 147:89–104
 47. Luo BH, Carman CV, Springer TA (2007) Structural basis of integrin regulation and signaling. *Annu Rev Immunol* 25:619–647
 48. Degryse B, Resnati M, Czekay RP, Loskutov DJ, Blasi F (2005) Domain 2 of the urokinase receptor contains an integrin-interacting epitope with intrinsic signaling activity: generation of a new integrin inhibitor. *J Biol Chem* 280:24792–24803
 49. Chaurasia P, Aguirre-Ghiso JA, Liang OD, Gårdsvoll H, Ploug M, Ossowski L (2006) A region in urokinase plasminogen receptor domain III controlling a functional association with

- alpha5beta1 integrin and tumor growth. *J Biol Chem* 281:14852–14863
50. Kucia M, Jankowski K, Reza R, Wysoczynski M, Bandura L, Allendorf DJ, Zhang J, Ratajczak J, Ratajczak MZ (2004) CXCR4-SDF-1 signalling, locomotion, chemotaxis and adhesion. *J Mol Histol* 35:233–245
51. Epstein RJ (2004) The CXCL12-CXCR4 chemotactic pathway as a target of adjuvant breast cancer therapies. *Nat Rev Cancer* 4:901–909
52. Waugh DJ, Wilson C, Seaton A, Maxwell PJ (2008) Multi-faceted roles for CXCR4-chemokines in prostate cancer progression. *Front Biosci* 13:4595–4604
53. Wong D, Korz W (2008) Translating an antagonist of chemokine receptor CXCR4: from bench to bedside. *Clin Cancer Res* 14:7975–7980
54. de Bock CE, Wang Y (2004) Clinical significance of urokinase-type plasminogen activator receptor (uPAR) expression in cancer. *Med Res Rev* 24:13–39
55. Sidenius N, Blasi F (2003) The urokinase plasminogen activator system in cancer: recent advances and implication for prognosis and therapy. *Cancer Metastasis Rev* 22:205–222
56. Pillay V, Dass CR, Choong PF (2007) The urokinase plasminogen activator receptor as a gene therapy target for cancer. *Trends Biotechnol* 25:33–39